

## Original Article

# Radiation engenders converse migration and invasion in colorectal cancer cells through opposite modulation of ANXA2/AKT/GSK3 $\beta$ pathway

Han Pan<sup>1</sup>, Yimeng Song<sup>1</sup>, Hang Zhang<sup>1</sup>, Yang Bai<sup>1</sup>, Teruaki Konishi<sup>2,3</sup>, Alisa Kobayashi<sup>2,3</sup>, Chunlin Shao<sup>1</sup>, Yan Pan<sup>1</sup>

<sup>1</sup>Institute of Radiation Medicine, Shanghai Medical College, Fudan University, No. 2094 Xie-Tu Road, Shanghai 200032, China; <sup>2</sup>Institute for Quantum Life Science, National Institutes for Quantum and Radiological Science and Technology, Inage, Chiba 263-8555, Japan; <sup>3</sup>National Institute of Radiological Sciences, National Institutes for Quantum and Radiological Science and Technology, Inage, Chiba 263-8555, Japan

Received September 2, 2020; Accepted October 20, 2020; Epub January 1, 2021; Published January 15, 2021

**Abstract:** Radiation therapy is an effective non-surgical means to achieve local control for various solid tumors including colorectal cancer (CRC), but metastasis and recurrences after conventional radiotherapy remains a major obstacle in clinical practice, and the knowledge concerning the changes of metastatic potential after heavy ion radiation is still limited. This study investigated how radiation, including  $\gamma$ - and carbon ion radiation, would change the metastatic capacity of two CRC cell lines, HCT116 and DLD-1, and examined the underlying molecular mechanisms. We found that the migration and invasion was enhanced in DLD-1 cells but impaired in HCT116 cells in vitro and in vivo after radiation of  $\gamma$ -rays or carbons, and radiation induced epithelial mesenchymal transition (EMT) in DLD-1 cells but mesenchymal epithelial transition (MET) in HCT116 cells. The expression of snail, a key inducer of EMT, was significantly enhanced by inhibition of glycogen synthase kinase-3 $\beta$  (GSK3 $\beta$ ) in both cell lines, suggesting the modulation of snail was alike in the two CRC cell lines. However, radiation inactivated GSK3 $\beta$  through stimulating the phosphorylation of AKT and GSK3 $\beta$  at Ser473 and Ser9 in DLD-1 cells respectively, but activated GSK3 $\beta$  by decreasing the expression of pAKT<sup>Ser473</sup> and pGSK3 $\beta$ <sup>Ser9</sup> or increasing the phosphorylation of GSK3 $\beta$  at Tyr216 in HCT116 cells. Therefore, the above inverted motility changes was due to the opposite modulation of AKT/GSK3 $\beta$  signaling pathway by radiation, which was further verified in other type of cancer cell lines including MCF-7, U251 and A549 cells. Moreover, it was found that annexin A2 (ANXA2) directly bound with GSK3 $\beta$  and acted as a negative regulator of GSK3 $\beta$  upon radiation. Knocking-down ANXA2 gene reversed the enhanced migration of the irradiated DLD-1 cells and strengthened radiation-impaired migration of HCT116 cells. Collectively, this study reveals that the change of cellular motility after radiation is independent of radiation type but is correlated with the inherent of cells.

**Keywords:** Colorectal cancer cells, radiation, migration and invasion, EMT, ANXA2/GSK3 $\beta$

## Introduction

Colorectal cancer (CRC) is one of the most prevalent cancer worldwide, which ranks third among all cancers in terms of incidence and second in terms of mortality [1]. CRC patients often present with overt metastases (~20%) or develop metastasis (20%-50%) during disease progression [2, 3]. Local invasion and distant metastasis of tumor cells are the main cause of CRC related death. Currently, surgical resection is still the main clinical treatment for CRC [4], however only 10%-20% of patients are candidates for curative resection.

Radiotherapy is one of the most common therapeutic approaches in clinical oncology. Conventional radiotherapy, including the treatments of  $\gamma$ -ray, X-ray and electron beam, has proved its benefits on overall survival in numerous types of cancers. For CRC, accumulating evidence indicates that radiotherapy can provide similar benefits to surgery in CRC. For example, local control up to 92% at 2 years can be achieved with stereotactic body radiation therapy (SBRT) in the treatment of oligometastatic CRC [5]. However, as a low-LET radiation, SBRT has limitation in cell killing efficiency due to the nature of X-ray. It is now clear that X-ray

or  $\gamma$ -ray radiation can either promote (in most cases) or inhibit the metastatic potential of malignance, as observed in various types of tumor cell lines [6], so the recurrence or distant metastases after local treatment with photon radiation remains a major therapeutic challenge. In contrast, high energy carbon ion (C-ion) radiation offers substantial potential clinical advantages over photon radiation due to its high relative biological effectiveness (RBE), low oxygen enhancement ratio (OER) and less variation in cell cycle related radiosensitivity. Now the heavy ion therapy has been expected to improve the clinical outcome of CRC patients. Hirokazu *et al.* reported that after C-ion radiotherapy, the 3-year actuarial overall survival rate approached to 78% for 29 CRC patients who could not receive resection, and the median survival time was 65 months [7]. An investigation of C-ion radiotherapy for pelvic recurrence of rectal cancer from 180 patients showed that the local control and survival rates at 5 years were 88% and 59%, respectively [8]. Unexpectedly, a few studies reported that C-ions could not hamper the motility of glioblastoma cells [9] or even be pro-invasive in pancreatic cancer cells [10]. These uncertainties highlight the necessity to unravel the remaining unknown mechanisms involved in the changes of metastasis potential after conventional and C-ion radiation.

Induction of epithelial mesenchymal transition (EMT) is closely related to the distant metastasis in tumor progression. Conventional radiation-mediated EMT has been widely studied in various types of tumors both *in vitro* and *in vivo* [11-13]. However, the role of C-ion radiation in EMT remains largely an unexplored area. In addition, the serine/threonine kinase, glycogen synthase kinase-3 $\beta$  (GSK3 $\beta$ ) is a positive regulator of cancer cell proliferation and survival in advanced cancer. Recently, it is shown that GSK3 $\beta$  controls EMT process and tumor metastasis by the degradation of slug [14] and dual regulation of snail [15], both are key transcription factors for EMT induction. Inhibition of GSK3 $\beta$  could preferentially attenuate the survival and proliferation of multiple types of tumor cells but induced EMT [16, 17] which may increase tumor invasion. Therefore, the role in regulating cell motility and EMT process after different types of radiation needs to be clarified.

Annexin A2 (ANXA2) is a calcium-dependent phospholipid-binding protein and belongs to a

highly conserved protein family of Annexins, and it can modulate multiple cell activities including proliferation, adhesion, migration, invasion and angiogenesis. Overexpression of ANXA2 is linked to tumorigenesis in many types of tumors including CRC [18]. Moreover, the increase of ANXA2 has been correlated with rapid recurrence and metastasis, poor response to chemotherapy and poor prognosis [19]. However, its role in radiation associated cell behavior remains unknown.

Here, we found that the migration and invasion potential was promoted in DLD-1 cells but decreased in HCT116 cells after  $\gamma$ - or C-ion radiation, and radiation induced EMT in DLD-1 cells, but mesenchymal epithelial transition (MET) in HCT116 cells. Further investigation revealed that the above converse motility changes in the two CRC cells was attributed to the opposite modulation of ANXA2/AKT/GSK3 $\beta$  signaling pathway after radiation, which was further confirmed in other cancer type cell lines. Moreover, we identified that ANXA2 bound directly with GSK3 $\beta$  and acted as a negative regulator of the activation of GSK3 $\beta$ . Knocking-down ANXA2 gene reversed the enhanced migration in the irradiated DLD-1 cells and in the meantime strengthened radiation-impaired migration in HCT116 cells.

### Methods and materials

#### Cell culture

Human CRC cell lines DLD-1, HCT116, lung cancer cell line A549 and breast cancer cell line MCF-7 were purchased from Shanghai Cell Bank. Radioresistant glioblastoma cell line U251R were previously established from its parental cell line U251 in our laboratory by exposing to 2 Gy X-ray/day (0.883 Gy/min) for 30 fractions (5 fractions/weekly in general) with a total dose of 60 Gy [20]. All cells were maintained in RPMI-1640 and DMEM (Hyclone Co., Beijing, China) medium, respectively, supplemented with 10% fetal bovine serum (FBS) (Gibco, Invitrogen, CA, USA), 100 U/ml penicillin and 100  $\mu$ g/ml streptomycin in a humidified atmosphere of 5% O<sub>2</sub> at 37°C.

#### Cell irradiation

Carbon ion irradiation was conducted at Heavy Ion Medical Accelerator of National Institute of Radiological Sciences in Japan [21]. The

## Radiation engenders converse migration in different cells

290-MeV/u mono energetic carbon ion beam with a LET of 70 keV/mm was used at an average dose rate of 0.5-1 Gy/min. Cells were also irradiated with  $\gamma$ -rays at a dose rate of 0.73 Gy/min using a  $^{137}\text{Cs}$   $\gamma$ -irradiator (Gammacell-40, Nordion Inc., Toronto, Canada) at room temperature.

### *Cell proliferation assay*

Cell proliferation was measured using a Cell Counting Kit-8 (CCK8) assay (Dojindo Laboratories, Kumamoto, Japan) as described previously [22]. Briefly, after different treatment, 2000 cells were seeded and grew for 6 days before the cell viability was determined. CCK-8 assay of cell proliferation was repeated four times with eight replicates for each cell sample.

### *Drug treatment*

Lithium chloride (LiCl, Sinopharm Chemical Reagent Co., Ltd., China) was dissolved in ddH<sub>2</sub>O and sterilized through a 0.22- $\mu\text{m}$  filter to have a stock solution. To inhibit the activity of GSK-3 $\beta$ , cells were pretreated with 40 mM LiCl for 5 h before exposure to other treatments.

### *Migration and invasion assays in vitro*

Cell migration and invasion were determined with wound healing and transwell assay. For the wound healing assay, MCF-7 cells were grown till full confluence, then exposed to 3 Gy of  $\gamma$ -radiation and scratched using a 200  $\mu\text{L}$  pipette tip. The cells was subsequently maintained in serum-free medium and photographed after 0 h and 48 h of wound formation. The cell coverage area compared to the initial scratch wound was quantified using ImageJ software and defined as migration rate.

The migration and invasion assays for DLD-1, HCT116, U251R and A549 cells were performed using a 24-well transwell chamber (Corning, NY, USA) with an 8- $\mu\text{m}$ -pore PET membrane as described before [23]. The invasion and migration of cells was photographed at 40 $\times$  magnification in order to cover ~90% of the bottom surface of the transwell. The extents of invasion and migration were determined by counting cells at 200 $\times$  magnification in at least 8 different fields of each well and were expressed as the average number of cells per field.

### *Mouse model for in vivo metastasis assay*

Male BALB/c nu/nu mice (Slac laboratory animal center, Chinese Academy of Science, Shanghai, China) in 4-5 weeks old were used for tumor metastasis assay. Control or irradiated (3 Gy) CRC cells ( $3 \times 10^6$  cells in 100  $\mu\text{l}$  of 0.9% NaCl solution) were injected into mice through tail vein. After 8 weeks, all the mice were anesthetized with ketamine and sacrificed by cervical dislocation and the lungs from each mouse were dissected and stained with Bouin's solution. The number of macroscopically visible pulmonary metastatic nodules was then counted. All *in vivo* experiments were repeated twice and carried out in accordance with the guidelines issued by the Institutional Animal Care and Use Committee.

### *Western blot assay*

Whole cell protein extracts were analyzed by western-blot assay as described before [24]. The primary antibodies were anti-E-cadherin, anti-N-cadherin, anti-snail, anti-vimentin, anti-phosphorylated GSK3 $\beta$  (p-Ser9 or p-Tyr216), anti-ANXA2 (1:1000, Cell Signaling Technology), and anti-phosphorylated AKT (p-Ser473) (1:1000; Abcam, Cambridge, MA). The proteins were detected by the enhanced chemiluminescence system (Millipore, Merck, German) and their band images were recorded by the Bio-Rad ChemiDoc XRS system and analyzed using the Quantity One software (Bio-Rad, Hercules, CA, USA). For the detection of proteins with similar or the same molecular weight, after the first chemiluminescence, the original antibody was stripped and the membrane was incubated with other antibodies.

### *Immunoprecipitation (IP) and label-free LC-MS/MS analysis*

Cell samples were lysed in an IP buffer (Beyotime Biotech., Haimen, China) containing protease inhibitor cocktails (Sigma, USA). The homogenates were incubated on ice for 45 min. Subsequently, the samples were centrifuged at 10000 g for 15 min at 4°C. The total cell lysates were incubated with GSK3 $\beta$  primary antibodies or IgG on protein G magnetic beads (Cell Signaling, USA) overnight. Then the immunoprecipitates were collected for label free LC-MS/MS measurement performed

## Radiation engenders converse migration in different cells

by Genechem Co., Ltd. (Shanghai, China) and western blot assay.

### *Immunofluorescence staining*

Immunofluorescence assay of ANXA2 was carried out as described before [25]. Briefly, after the indicated treatments, cells were fixed *in situ* with 4% paraformaldehyde for 15 min and permeabilized with the enhanced immunostaining permeabilization buffer (Beyotime Biotech.) for 5 min at room temperature. Then the non-specific sites were blocked at room temperature for 1 h and the cells were incubated with the primary anti-ANXA2 antibody at a dilution of 1:100 at 4°C overnight. Subsequently, cells were incubated with the secondary antibodies anti-IgG rabbit Alexa Fluor®555 (Thermo Fisher Scientific, USA) at 1:600 in the dark for 1 h and then the cell nuclei were counterstained with DAPI (5 µg/ml) for 5 min. The samples were examined and recorded using a fluorescence microscope (Olympus, Japan).

### *RNA interference*

Specific knockdown of ANXA2 was achieved using two siRNA oligonucleotides with the following sequences, ANXA2 #1: 5-CGG GAT GCT TTG AAC ATT GAA-3, and ANXA2 #2: 5-TG-AGGGTGACGTTAGCATTAC-3. Cells were transfected with 40 nM siRNA using RNAiMAX (Thermo, USA) 24 h before radiation according to the manufacturer's introduction. The efficiency of siRNA knockdown was checked using western blot assay 48 h after transfection.

### *Statistical analysis*

All cellular experiments were repeated independently at least three times with three to four replicates. Data are presented as means ± SE. Comparison is performed by two-sample student's t-test.  $P < 0.05$  was considered as statistically significant.

## Results

### *Effects of $\gamma$ -ray or C-ion radiation on the migration and invasion of DLD-1 and HCT116 cells*

**Figure 1A** and **1B** illustrated that the viabilities of DLD-1 and HCT116 cells were significantly reduced by  $\gamma$ -ray or carbon ion radiation in a

dose-dependent manner, and DLD-1 cells were more radioresistant than HCT116 cells. Then we detected the migration and invasiveness of the two cell lines after 3 or 6 Gy  $\gamma$ -radiation. Interestingly, **Figure 1C** showed that  $\gamma$ -radiation significantly promoted the migration and invasiveness of DLD-1 cells, in contrast, it inhibited the migratory and invasive capacity of HCT116 cells. Then DLD-1 and HCT116 cells were exposed to C-ions of 0.5 or 1 Gy dose, which rendered similar cell viability as exposed to the above  $\gamma$ -radiation. We supposed that the increased migration and invasiveness of DLD-1 cells could be eliminated or reversed by heavy ion radiation, however, as shown in **Figure 1D**, C-ion radiation still enhanced the migratory and invasive potential of DLD-1 cells, although the increased number of migration cells was lower than  $\gamma$ -radiation, and in the meantime it significantly decreased the migration and invasiveness of HCT116 cells.

The *i.v.* model was then applied to test the metastatic ability of the irradiated CRC cells. As shown in **Figure 1E** and **1F**, two months after *i.v.* injection, 100% mice (10/10) injected with 3 Gy  $\gamma$ -ray irradiated DLD-1 cells developed metastatic lung lesions and the average number of nodules per lung was  $16 \pm 2$ , whereas 6 out of 7 mice injected with non-irradiated DLD-1 cells developed lung metastasis and the average number of nodules per lung was  $6 \pm 2$ . For HCT116 cells, 6 out of 9 mice injected with 3 Gy  $\gamma$ -ray irradiated cells developed lung metastasis and the average number of metastatic nodules per lung was only  $4 \pm 1$ , whereas all mice injected with non-irradiated cells had lung metastasis and the average number of metastatic nodules per lung increased to  $13 \pm 2$ . Accordingly, radiation increased the metastatic ability of DLD-1 cells but decreased the metastasis of HCT116 cells *in vivo*.

### *Effects of $\gamma$ -ray or C-ion radiation on EMT process of DLD-1 and HCT116 cells*

EMT is known to play critical and intricate roles in tumor invasion and metastasis of various types of cancers, thus we checked the expression of EMT-related proteins in these two CRC cells. As shown in **Figure 2A**, a typical EMT phenotype including decreased-expression of E-cadherin and up-regulation of N-cadherin,

## Radiation engenders converse migration in different cells

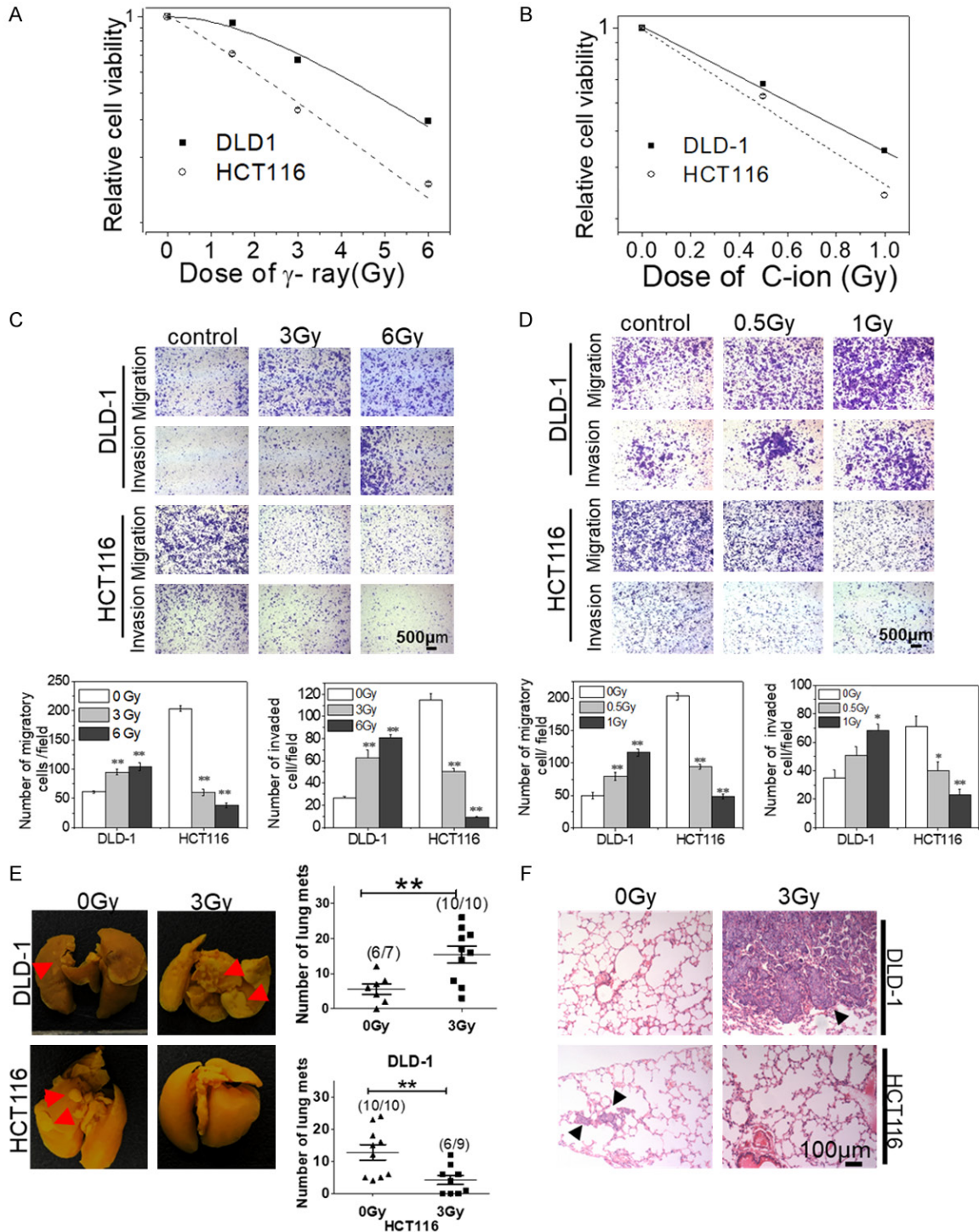


**Figure 1.** Radiation induced converse migration and invasion capability in DLD-1 and HCT116 cells *in vivo* and *in vitro*. (A, B) Relative cell viability of HCT116 and DLD-1 cells after high or low-LET radiation, (A)  $\gamma$ -radiation, (B) C-ion radiation. (C, D) Effects of  $\gamma$ -radiation (C) or C-ion radiation (D) on the migration and invasiveness of DLD-1 and HCT116 cells. Migration and invasion were assayed using transwell coated with or without matrigel, and the photographs are the representative images of the migratory and invaded cells of DLD-1 and HCT116 cells. Data represent the mean  $\pm$  SE for at least three independent experiments. (E) Lung metastasis from i.v. injected DLD-1 or HCT116 cells with or without 3 Gy of  $\gamma$ -radiation before injection. Data represent the mean  $\pm$  SE generated from 2 independent experiments with 7-10 mice/group. (F) Images of H&E staining of lungs from i.v. injected DLD-1 or HCT116 cells with or without 3 Gy of  $\gamma$ -radiation before injection. Arrows show the typical lung metastases. \* $P < 0.05$  and \*\* $P < 0.01$  compared with non-irradiated group.

## Radiation engenders converse migration in different cells

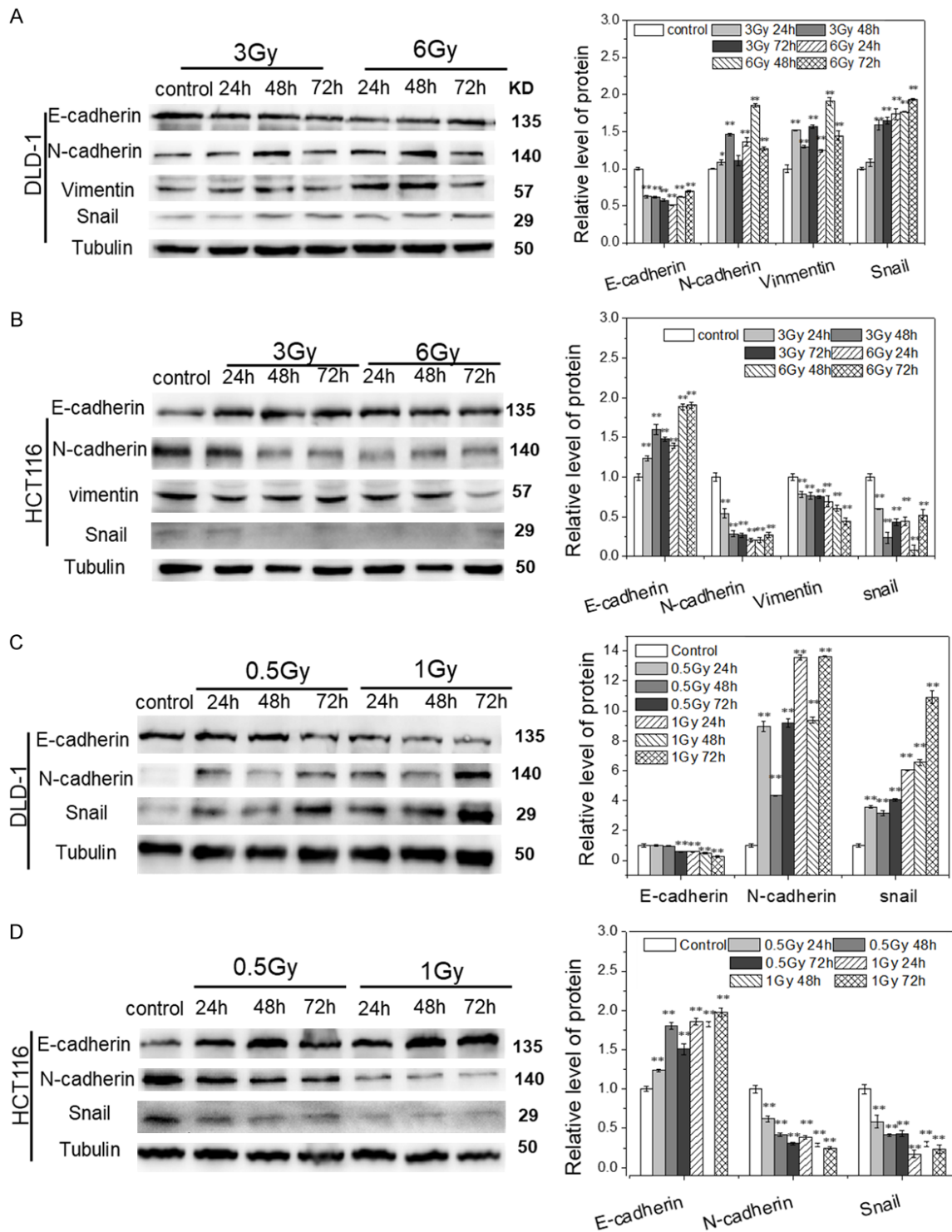


**Figure 2.** Carbon ion or  $\gamma$ -radiation triggers EMT in DLD-1 but MET in HCT116 cells. (A, B) Expressions of EMT-related proteins 24-72 h in DLD-1 (A) and HCT116 (B) cells after  $\gamma$ -radiation. (C, D) Expression of EMT-related proteins in DLD-1 (C) and HCT116 (D) cells at 24-72 h after C-ion radiation. The original uncropped gels of Western blot assay were shown in [Supplementary Figure 1](#). The column plots show the relative amounts of E-cadherin, N-cadherin, Vimentin and snail that were normalized to tubulin first and then the ratio of each normalized value to the control value was calculated. Data were generated from at least three independent experiments. \* $P < 0.05$  and \*\* $P < 0.01$  compared with non-irradiated control.

## Radiation engenders converse migration in different cells

vimentin and snail was identified in DLD-cells at 24-72 h after 3 Gy and 6 Gy of  $\gamma$ -radiation. In contrast, a typical MET phenotype, which is shown as increased expression of E-cadherin and down-regulated N-cadherin, vimentin and snail was observed in the irradiated HCT116 cells (**Figure 2B**). Similarly, the expression of E-cadherin was down-regulated and the expressions of N-cadherin and snail were elevated in the C-ion irradiated DLD-1 cells, but all of these proteins in C-ion irradiated HCT116 cells had opposite expression patterns in comparison with DLD-1 cells (**Figure 2C, 2D**). Taken together, the converse migration and invasion behaviors of the irradiated DLD-1 and HCT116 cells may result from their EMT or MET alteration after radiation.

### *Inhibition of GSK3 $\beta$ stimulated the migration and invasion of the irradiated CRC cells by regulating snail expression*

Snail is a key transcription factor of EMT and plays critical role in CRC progression. Since GSK3 $\beta$  can negatively regulate the stabilization of snail [15], we wonder whether GSK3 $\beta$  impacts EMT process in the irradiated CRC cells. **Figure 3A** and **3B** showed that LiCl, a potent inhibitor of GSK3 $\beta$ , strongly increased the expressions of snail and N-cadherin in HCT116 and DLD-1 cells, indicating that GSK3 $\beta$  inversely regulated snail protein level in both cell lines. Meanwhile, **Figure 3C** showed that inhibition of GSK3 $\beta$  significantly increased the migratory and invasive potential in DLD-1 cells with or without radiation, but it effectively weakened the radiation suppressed migration and invasion in HCT116 cells, compared to those without LiCl treatment.

Since the above results indicated that the regulation of snail by GSK3 $\beta$  was alike in two CRC cell lines, we speculate that the cause of the inverted cellular behavior in the irradiated DLD-1 and HCT116 cells may lie in the upstream modulation of GSK3 $\beta$  activity.

### *Radiation conversely modulated the activity of GSK3 $\beta$ through AKT pathways in two CRC cell lines*

To test the above hypothesis, we determined the activity of GSK3 $\beta$  in two CRC cell lines after radiation. It is known that GSK3 $\beta$  can be phosphorylated by AKT at Ser9, which renders

GSK3 $\beta$  an inactive form, while Tyr216 phosphorylation inactivates GSK3 $\beta$ . **Figure 4A** showed that, after  $\gamma$ -radiation, the expression of p-AKT<sup>Ser473</sup> was increased in accompany with the up-regulation of p-GSK3 $\beta$ <sup>Ser9</sup> but no detectable change of p-GSK3 $\beta$ <sup>Tyr216</sup> in DLD-1 cells could be observed. While in HCT116 cells, the expression of p-AKT<sup>Ser473</sup> was significantly decreased in accompany with a drastic increase of p-GSK3 $\beta$ <sup>Tyr216</sup> expression but the level of p-GSK3 $\beta$ <sup>Ser9</sup> did not change significantly in comparison with their non-irradiated control (**Figure 4B**). We further detected the changes of the phosphorylation of these proteins after C-ion radiation and found that the expression of p-AKT<sup>Ser473</sup> and p-GSK3 $\beta$ <sup>Ser9</sup> were increased in DLD-1 cells but obviously decreased in HCT116 cells, which had similar trend with that after  $\gamma$ -radiation (**Figure 4C, 4D**).

### *Effect of radiation on the migration of U251, A549 and MCF-7 cells*

To broaden our findings, we tested radiation-induced migration in other three cell lines, including radioresistant glioblastoma cell line U251R, lung adenocarcinoma cell line A549 and breast cancer cell line MCF-7. As shown in **Figure 5A**, the number of the migratory cells from U251R was much higher than its parental counterpart. Similarly, radiation obviously increased the migration of A549 cells (**Figure 5B**). In contrast, the migratory capacity was significantly impaired in the irradiated MCF-7 cells in comparison with its unirradiated control (**Figure 5C**). In addition, the expressions of p-AKT<sup>Ser473</sup> and p-GSK3 $\beta$ <sup>Ser9</sup> were increased in U251R cells and the irradiated A549 cells, while the expressions of p-GSK3 $\beta$ <sup>Tyr216</sup> had no alteration. However, in MCF-7 cells, radiation significantly increased the expression of p-GSK3 $\beta$ <sup>Tyr216</sup> but decreased the phosphorylation of p-AKT and p-GSK3 $\beta$  at Ser473 and Ser9, respectively. These results were consistent with that in DLD-1 and HCT116 cells respectively, i.e., these data validated our findings concerning CRC migration in other tumor type cells.

### *Identification of ANXA2 that can bind with GSK3 $\beta$ in CRC cells*

Next, endogenous GSK3 $\beta$  was immunoprecipitated in HCT116 and DLD-1 cells at 24 h after  $\gamma$ -radiation, and the obtained protein complex-

## Radiation engenders converse migration in different cells

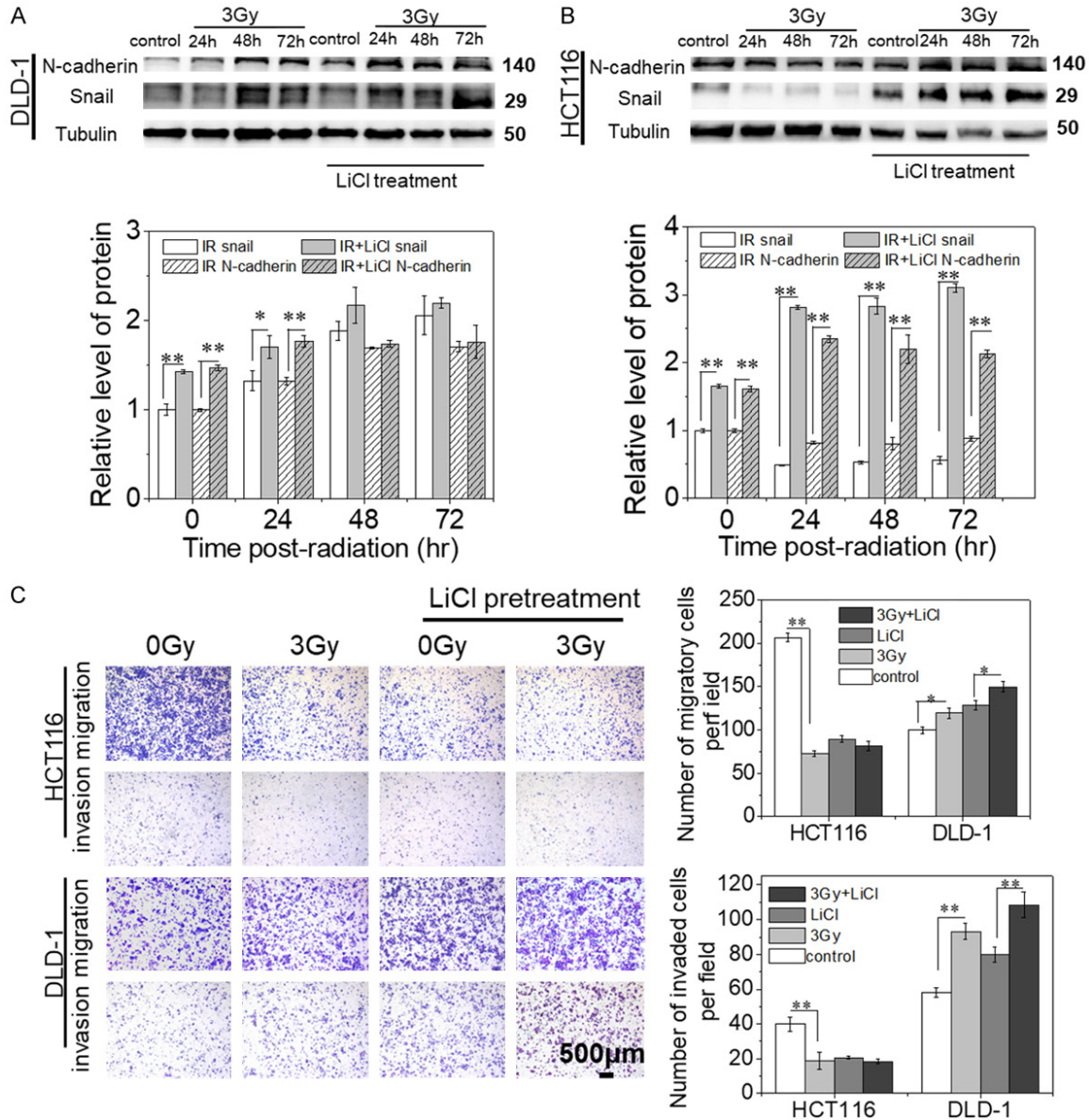


**Figure 3.** Inhibition of GSK3 $\beta$  stimulates the migration and invasion of DLD-1 and HCT116 cells after  $\gamma$ -radiation. (A, B) LiCl promoted the expressions of N-cadherin and snail in DLD-1 cells (A) and HCT116 (B) cells. The original uncropped gels of Western blot assay were shown in [Supplementary Figure 2](#). The column plot shows the relative amounts of N-cadherin and snail that were normalized to tubulin first and then the ratio of each normalized value to the control value was calculated. (C) LiCl pretreatment promoted radiation-enhanced migration and invasion in DLD-1 cells and reversed radiation-decreased motility of HCT116 cells after 3 Gy of  $\gamma$ -radiation. The photographs are the representative images of the migration and invasion of DLD-1 and HCT116 cells. Data were generated from three independent experiments. \* $P < 0.05$  and \*\* $P < 0.01$  compared with the indicated control.

es were subject to LC-MS/MS analysis (**Figure 6A**). A total of 155 proteins were identified ([Supplementary Table 1](#)), among which ANXA2 is involved. GEPIA database analysis shows that ANXA2 is highly expressed in CRC tissue in comparison with normal mucosae (**Figure 6B**). Hence we speculated that ANXA2 might be a direct modulator of GSK3 $\beta$ . To verify this

assumption, the cellular protein extracts were detected by co-IP assay using GSK3 $\beta$  antibody followed by western blot assay. **Figure 6C** showed that ANXA2 was detected in GSK3 $\beta$  precipitates, indicating that ANXA2 binds with GSK3 $\beta$  directly. This protein interaction was further confirmed by a reciprocal experiment where the protein lysate was immunoprecipi-

## Radiation engenders converse migration in different cells

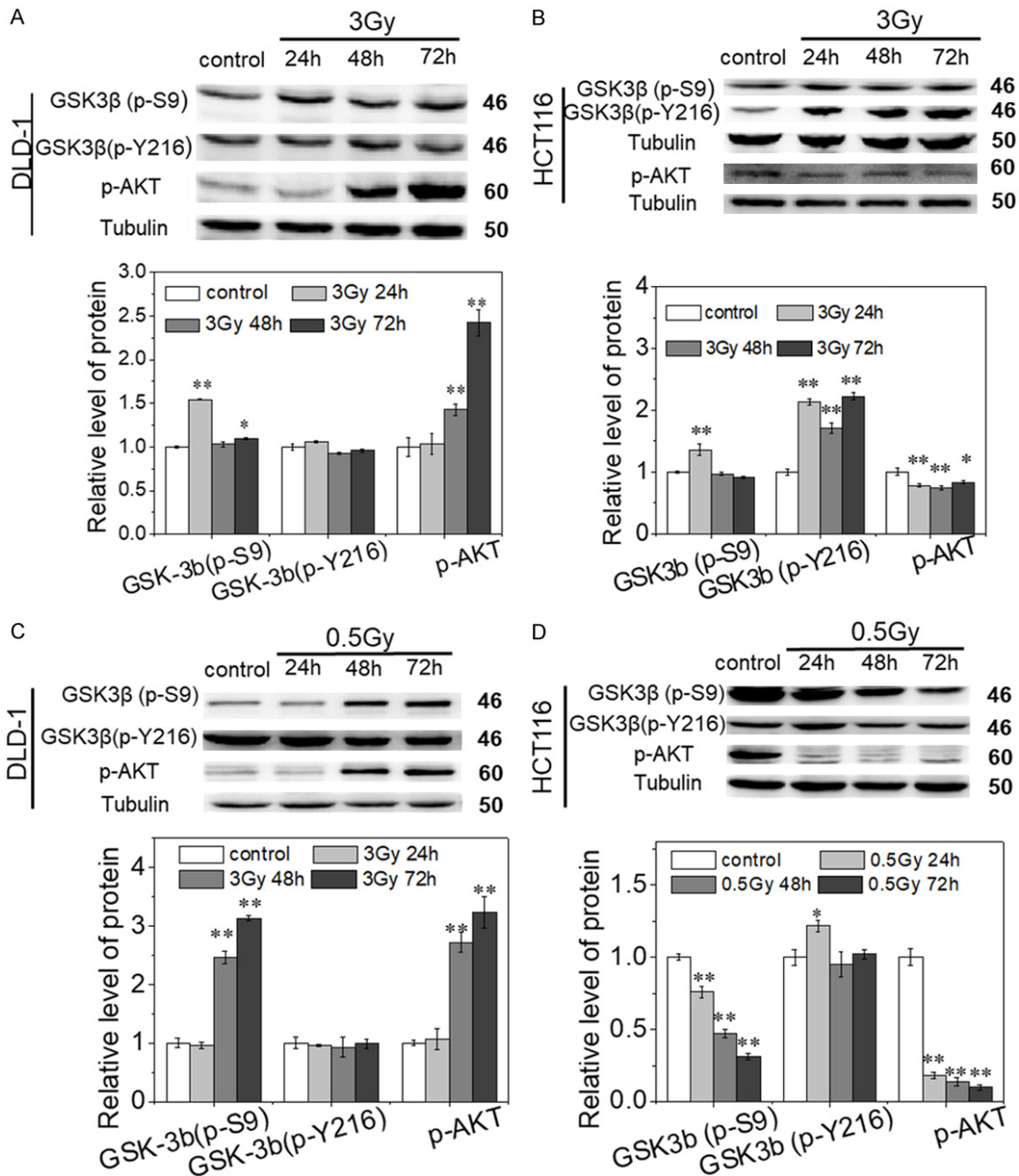
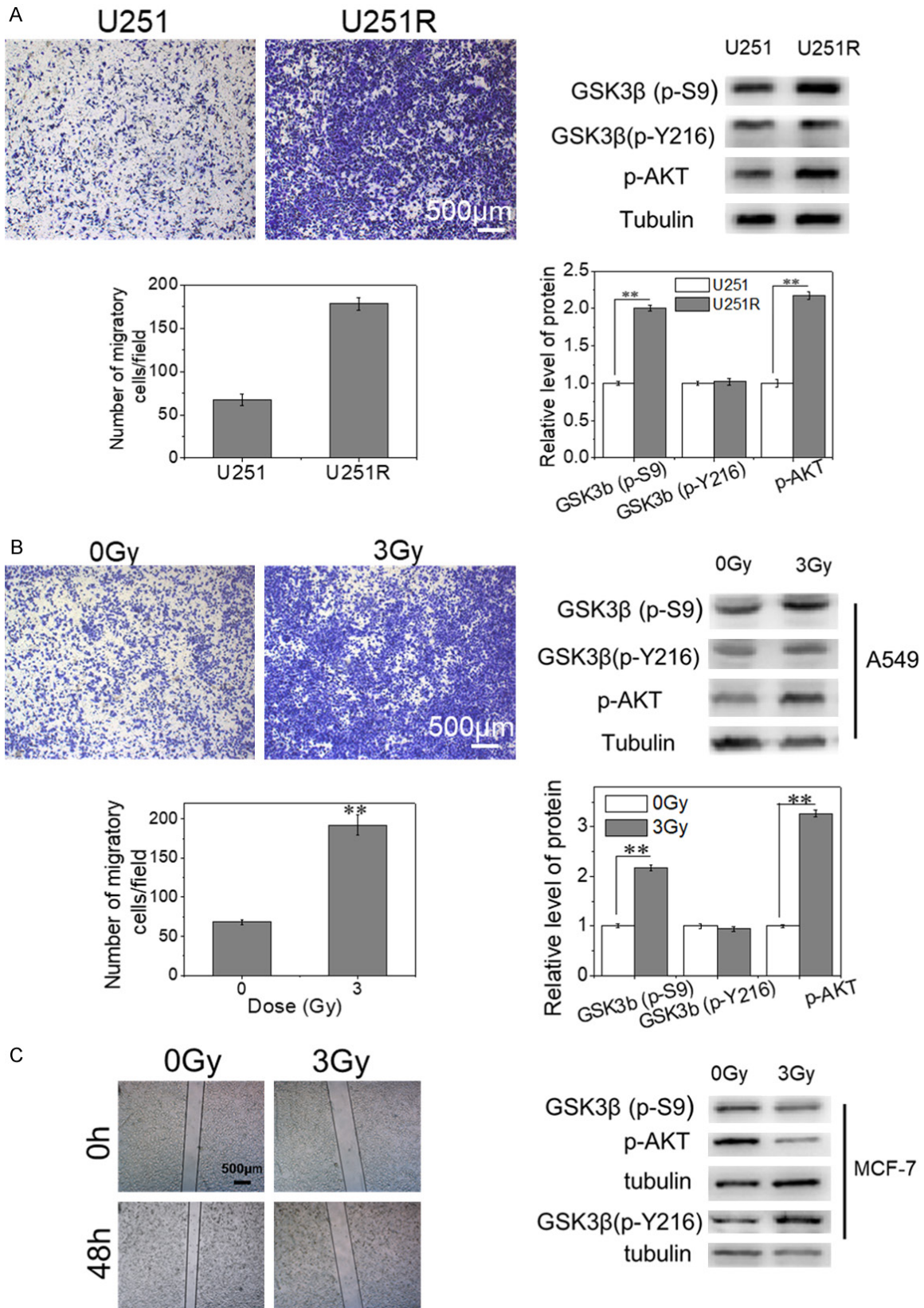


**Figure 4.** Carbon or  $\gamma$ -radiation conversely modulates the activity of GSK3 $\beta$  in DLD-1 and HCT116 through AKT pathway. (A, B) Expressions of p-GSK3 $\beta$  (Ser9 and Tyr216) and p-AKT (Ser473) in DLD-1 cells (A) and HCT116 cell (B) at 24-72 h after 3 Gy of  $\gamma$ -radiation. (C, D) Expressions of p-GSK3 $\beta$  (Ser9 and Tyr216) and p-AKT (Ser473) in DLD-1 cells (C) and HCT116 cells (D) at 24-72 h after 0.5 Gy of C-ion radiation. The original uncropped gels of Western blot assay were shown in [Supplementary Figure 3](#). The column plots show the relative amounts of phosphorylated GSK3 $\beta$  (Ser9 and Tyr216) and AKT (Ser473) that were normalized to tubulin first and then the ratio of each normalized value to the control value was calculated. Data were generated from three independent experiments. \* $P < 0.05$  and \*\* $P < 0.01$  compared with un-irradiated control.

tated by anti-ANXA2 monoclonal antibody and the binding protein was recognized by anti-GSK3 $\beta$  antibody (**Figure 6D**).

Then we wonder how ANXA2 responds toward radiation in HCT116 and DLD-1 cells. **Figure 6E** showed that, when cells were exposed to  $\gamma$ -rays

Radiation engenders converse migration in different cells



## Radiation engenders converse migration in different cells

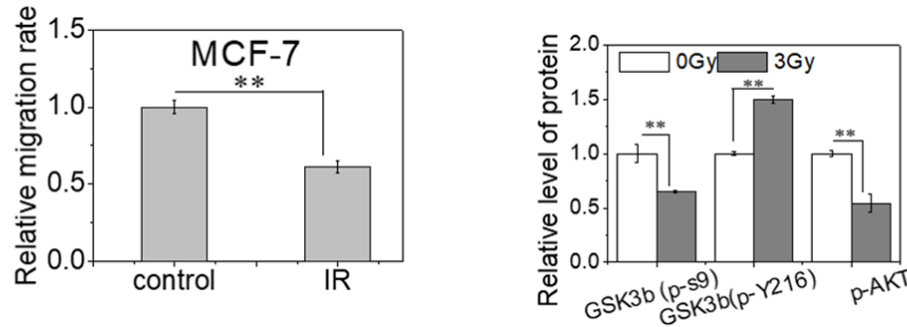


**Figure 5.** Effect of radiation on the migration of U251, A549 and MCF-7 cells. (A) The migration of U251 cells and its radioresistant subline U215R, and the expressions of p-AKT (Ser473), p-GSK3 $\beta$  (S9 and Y216) in U251 and U251R cells. (B, C) The effect of radiation on the migratory capacity of A549 (B) and MCF-7 (C) cells, and the expressions of p-AKT, p-GSK3 $\beta$  (S9 and Y216) in A549 and MCF-7 cells at 72 h after 3 Gy of  $\gamma$ -radiation. Cellular migration were detected using transwell (U251, U251R, and A549) or wound healing (MCF-7) assay. The original uncropped gels of Western blot assay were shown in [Supplementary Figure 4](#). The photographs are the representative images of the migration of U251, U251R, A549 and MCF-7 cells. The column plots show the number of migratory cells per field or the relative migration rate, and the relative amounts of phosphorylated GSK3 $\beta$  (Ser9 and Tyr216) and AKT (Ser473) that were normalized to tubulin first and then the ratio of each normalized value to the control value was calculated. Data were generated from three independent experiments. \* $P < 0.05$  and \*\* $P < 0.01$  compared with unirradiated control.

or C-ions, the expression of ANXA2 in DLD-1 cells increased significantly over time after radiation, while it slightly decreased in the irradiated HCT116 cells. Immunofluorescence staining also demonstrated the opposite changes of ANXA2 expression in these two CRC cell lines after radiation (**Figure 6F**).

### ANXA2 negatively regulate the activity of GSK3 $\beta$

The crosstalk between ANXA2 and GSK3 $\beta$  was then determined. As shown in **Figure 7A**, LiCl treatment did not alter the expression level of ANXA2 in HCT116 and DLD-1 cells whether they were irradiated or not, but the radiation-enhanced expressions of p-AKT<sup>Ser473</sup> and p-GSK3 $\beta$ <sup>Ser9</sup> were more prominent in LiCl-treated DLD-1 cells. While in HCT116 cells, the radiation-decreased expression of p-AKT<sup>Ser473</sup> was totally reversed by LiCl treatment. However, the original changes of p-GSK3 $\beta$ <sup>Tyr216</sup> in these two CRC cells after radiation were not altered. To further confirm the relationship between ANXA2 and AKT/GSK3 $\beta$ , the expression of ANXA2 was effectively knocked down in DLD-1 and HCT116 cells by ANXA2 siRNAs (**Figure 7B**). **Figure 7C** showed that, in comparison with the negative control (si-control), silencing ANXA2 significantly decreased the expressions of p-AKT<sup>Ser473</sup> and GSK3 $\beta$ <sup>Ser9</sup> at 24-72 h after radiation, but it did not change

the expression level of p-GSK3 $\beta$ <sup>Tyr216</sup> in DLD-1 cells. As for HCT116 cells, ANXA2 knock-down significantly reduced the expression of p-AKT<sup>Ser473</sup> and GSK3 $\beta$ <sup>Ser9</sup> but weakened the up-regulation of p-GSK3 $\beta$ <sup>Tyr216</sup> by radiation. Moreover, silencing ANXA2 drastically decreased the migratory capacity of both non-irradiated cell lines, and totally reversed radiation-enhanced migration in DLD-1 cells while significantly strengthened radiation impaired migration in HCT116 cells (**Figure 7D**).

### Discussion

It is well accepted that conventional radiation can paradoxically improve or impair the metastasis of various types of tumor cells [26]. In contrast, C-ion radiation is known to diminish the invasive potential of cancer cells *in vitro* and *in vivo* and has advantage over photon radiation [27, 28]. We found that  $\gamma$ -radiation can suppress the migration and invasion of HCT116 cells but strengthens the metastasis capacity of DLD-1 cells both *in vivo* and *in vitro*. Surprisingly, the increased motility was still observed in DLD-1 cells after C-ion radiation, although this beam decreased the migration and invasion in HCT116 cells. Similar to our findings, it was reported that the migration of HCT116 and MCF-7 cells significantly decreased after X-ray or C-ion radiation [29, 30]. Other literatures showed that C-ion radia-

## Radiation engenders converse migration in different cells

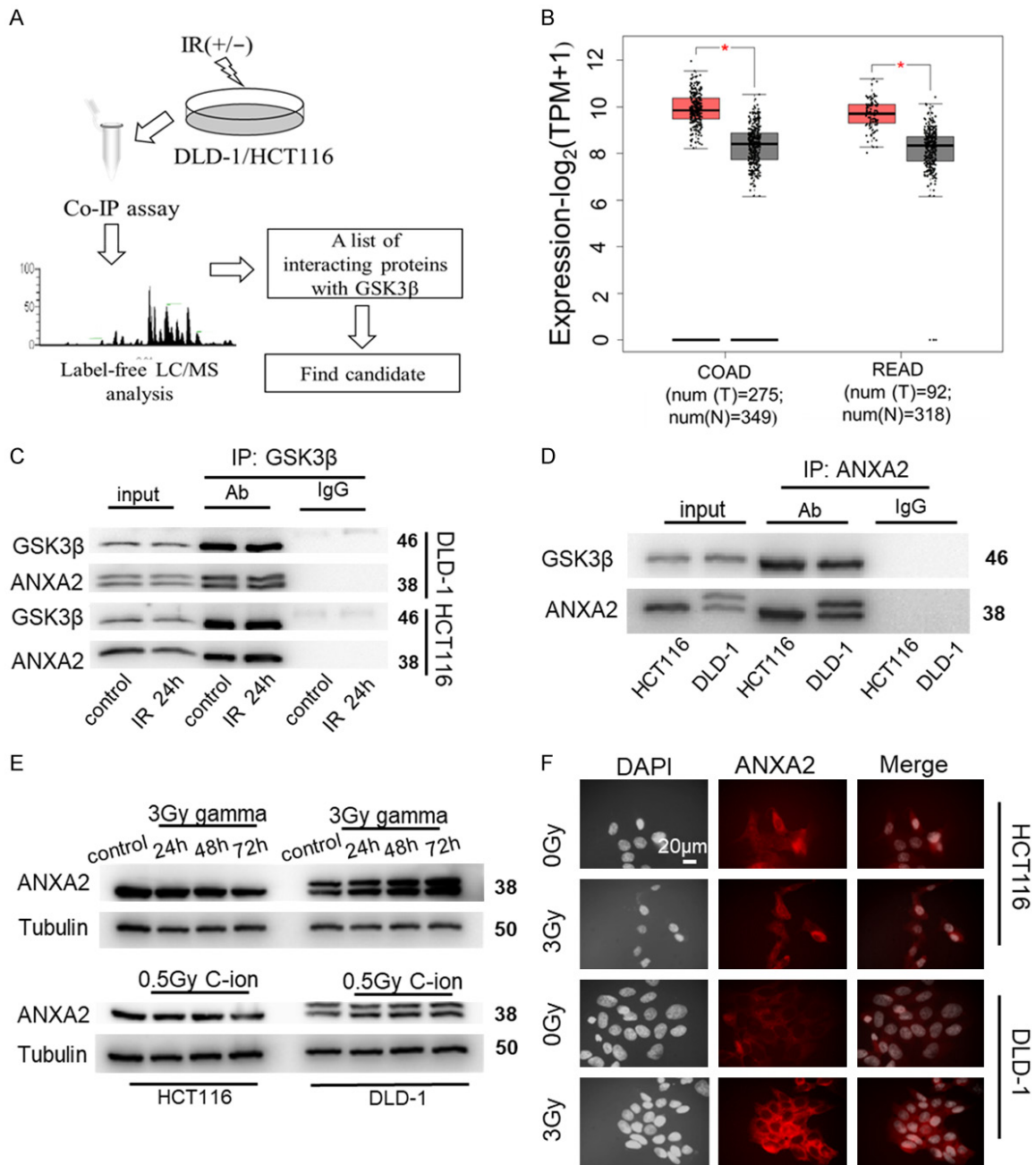


**Figure 6.** ANXA2 interacts directly with GSK3 $\beta$ . **A.** Experimental procedure to identify the proteins directly binding to GSK3 $\beta$ . **B.** Comparison of the expression of ANXA2 between tumor and normal tissue. **C.** Endogenous ANXA2 were detected by co-IP assay with anti-GSK3 $\beta$  antibody in DLD-1 and HCT116 cells. **D.** Endogenous GSK3 $\beta$  were detected by co-IP assay with anti-ANXA2 antibody in DLD-1 and HCT116 cells. **E.** Expression of ANXA2 in DLD-1 and HCT116 cells at 24-72 h after 3 Gy of  $\gamma$ -ray or 0.5 Gy of C-ion radiation. **F.** Fluorescent staining for ANXA2 in DLD-1 and HCT116 cells at 72 h after 0 or 3 Gy of  $\gamma$ -radiation. The original uncropped gels of Western blot assay were shown in [Supplementary Figure 5](#).

tion enhanced the invasive potential in A549 cells [31] and increased the metastatic rate in rats bearing prostate adenocarcinoma [32], which is consistent with our results in DLD-1 cells. Based on the above data, we speculate

that whether the motility of tumor cells is enhanced or decreased after radiation may be independent of radiation type but is correlated with the inherent of cells. Therefore, the comparison of molecular changes between

## Radiation engenders converse migration in different cells

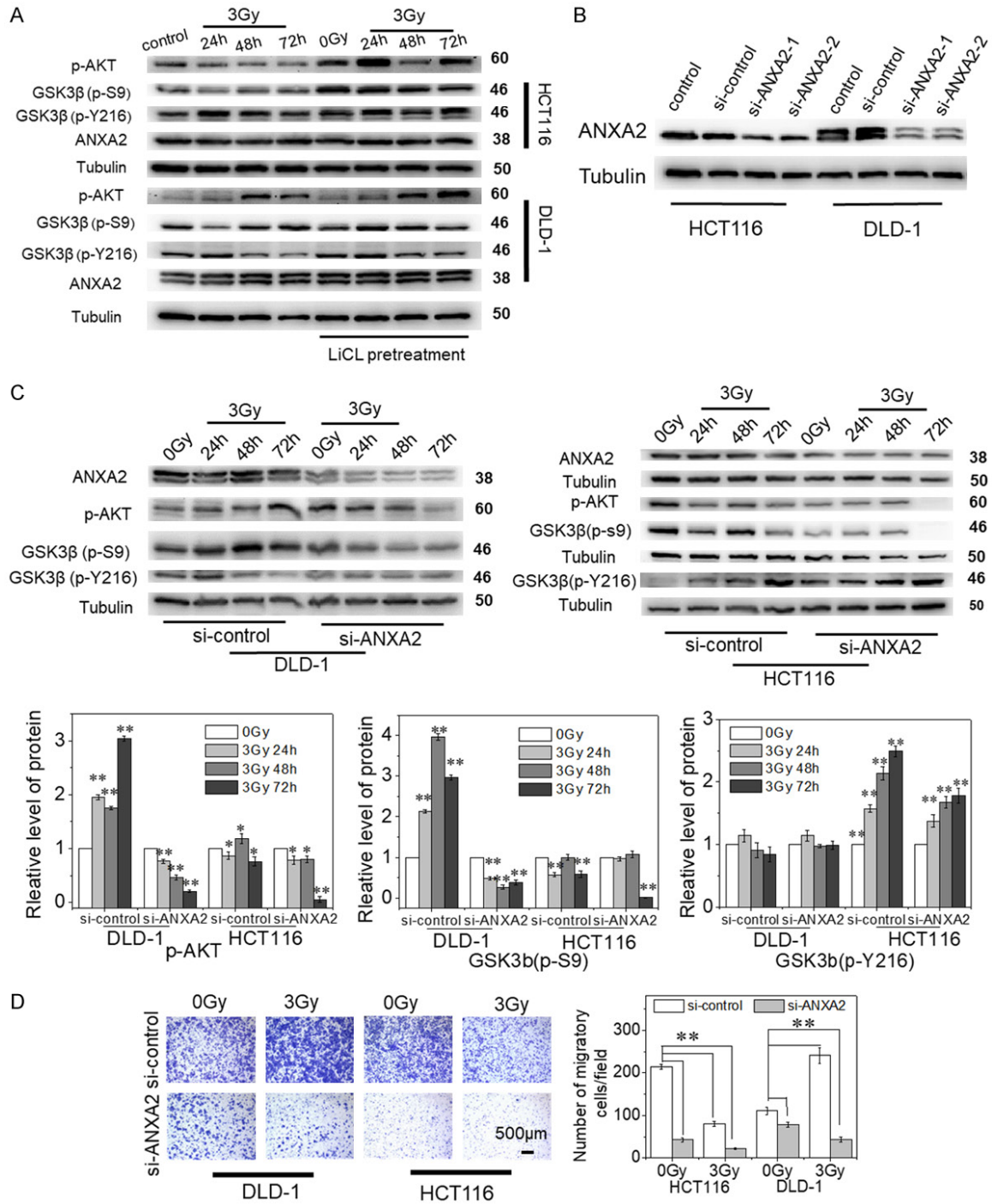


**Figure 7.** ANXA2 negatively regulates the activity of GSK3β upon radiation. **A.** Expressions of p-AKT (Ser473), p-GSK3β (S9 and Y216) and ANXA2 in DLD-1 and HCT116 cells at 24-72 h after 3 Gy of γ-radiation with or without LiCl pretreatment. **B.** The efficiency of ANXA2 knockdown was examined by western blot assay, both siRNAs against ANXA2 significantly decreased its expression in HCT116 and DLD-1 cells. **C.** Expressions of ANXA2, p-AKT (Ser473), p-GSK3β (S9 and Y216) in ANXA2 knockdown DLD-1 and HCT116 cells at 24-72 h after 3 Gy of γ-radiation. The original uncropped gels of Western blot assay were shown in [Supplementary Figure 6](#). The column plots show the relative amounts of the indicated proteins that were normalized to tubulin first and then the ratio of each normalized value to the control value was calculated. Data were generated from three independent experiments. \* $P < 0.05$  and \*\* $P < 0.01$  compared with the respective control. **D.** Representative images showing the migration of DLD-1 and HCT116 cells pretreated with siANXA2 or si-control followed by 3 Gy of γ-radiation, and the number of migratory cells per field were counted. Data were generated from three independent experiments. \* $P < 0.05$  and \*\* $P < 0.01$  compared with non-irradiated si-control.

## Radiation engenders converse migration in different cells

HCT116 and DLD-1 cells might yield critical information on the signaling pathways upon radiation and may allow for developing new clinical strategies to improve the outcome of radiotherapy.

EMT is a reversible biological process and closely involved in the initial cell-migratory phenotype in various neoplasia. Radiation can induce EMT and enhance metastasis in several kind of cancers but decrease the metastasis in other kinds of cancers [26, 33]. Consistent with the motility changes of the above two CRC cell lines, we found that C-ion or  $\gamma$ -ray radiation induced EMT in DLD-1 cells but induced MET in HCT116 cells (**Figure 2**). Of particular note, snail is a key factor that regulates EMT and an early marker of this program [34]. During EMT, snail represses E-cadherin transcription by directly binding to its promoter and activates the expressions of mesenchymal phenotype related proteins such as N-cadherin and vimentin [35]. Data mining from TCGA database showed that snail has the highest frequency of overexpression in colorectal cancer compared with other EMT-inducers including ZEB1, slug and ZEB2 [36], suggesting that snail may also play vital role in radiation-modulated EMT in our experiment. In the present study, we found that snail expression was elevated in DLD-1 cells but declined in HCT116 cells after C-ion or  $\gamma$ -radiation, indicating the inversed regulation of snail by radiation in these two CRC cell lines may be responsible for the above different changes of cell motilities.

GSK3 $\beta$  can phosphorylate snail and regulate its function in mediating EMT [15]. We found that the regulatory mechanism of snail by GSK3 $\beta$  was alike in the two CRC cell lines. When GSK3 $\beta$  was inhibited, the expression of snail was up-regulated and the migration and invasion were stimulated in both cell lines after radiation. In consistent with our findings, inactivation of GSK3 $\beta$  by LiCl treatment notably increased EMT of MCF-7 cells [37], abolished the suppression of cell invasion mediated by HOXA4 and increased the migration and invasion of lung cancer cells [38]. Hence, the likely possibility that radiation induced opposite expression patterns of snail in DLD-1 and HCT116 cells is due to the converse regulation of GSK3 $\beta$  in these CRC cells.

It is demonstrated that the activity of GSK3 $\beta$  is inhibited by the phosphorylation of Ser9

[39] but triggered by the phosphorylation at Try216 site [40]. Our results showed that  $\gamma$ -ray or C-ion radiation inactivated GSK3 $\beta$  in DLD-1 cells by up-regulating the phosphorylation of AKT, a mediator of GSK3 $\beta$ . Similarly, radiation inactivated GSK3 $\beta$  by phosphorylation of Ser9 and induced EMT in RLE-6TN cells [41]. In contrast, the same type and dose of radiation down-regulated p-AKT at Ser473 and then activated GSK3 $\beta$  in HCT116. More importantly, we verified these findings in other tumor type cells (**Figure 5A-C**). Therefore, the radiation-enhanced or decreased cellular motility is reasoned from the activation or inhibition of AKT/GSK3 $\beta$  signal pathway after radiation, which then changed the expression of snail and induced EMT or MET process.

Our another important finding is the identification of protein ANXA2 that negatively mediates GSK3 $\beta$  by directly binding to GSK3 $\beta$  protein. To the best of our knowledge, there is few literature reporting the relationship between these two proteins, except one paper reported that ANXA2 could bind to GSK3 $\beta$  and disrupt the formation of GSK3 $\beta$ / $\beta$ -catenin complex in hepatocarcinoma cells [42]. In addition, we found that the expression of ANXA2 was increased in DLD-1 but slightly decreased in HCT116 cells, which exhibited similar trend with the change of AKT/GSK3 $\beta$  pathway in the two CRC cells after radiation. The regulation between AKT and ANXA2 remains controversial. ANXA2 depletion could enhance the expression of p-AKT in H<sub>2</sub>O<sub>2</sub> treated HT1080 and MDA-MB231 cells [43], however other reports showed that ANXA2 activated AKT pathway [44] and ANXA2 knockdown inhibited p-AKT in the MHCC-97L cells [45]. In accordance, our results also demonstrated that silencing of ANXA2 impaired radiation-induced phosphorylation of AKT and increased the activation of GSK3 $\beta$  in DLD-1 cells. Notably, inhibition of GSK3 $\beta$  by LiCl had a feedback on the activation of p-AKT but had no effect on the expression of ANXA2, indicating ANXA2 was upstream of GSK3 $\beta$  and negatively regulated its activity upon radiation. Jurcak *et al.* reported a role for tumoral ANXA2 in the paracrine signaling mechanism of tumor cell migration toward nerves [46] and an increased expression of ANXA2 was detected in aggressive MDA-MB231 cells compared to non-invasive MCF-7 cells [47]. Consistently, silencing of ANXA2 in our experiment drastically decreased the migration of unirradiated CRC cells, reversed the

## Radiation engenders converse migration in different cells

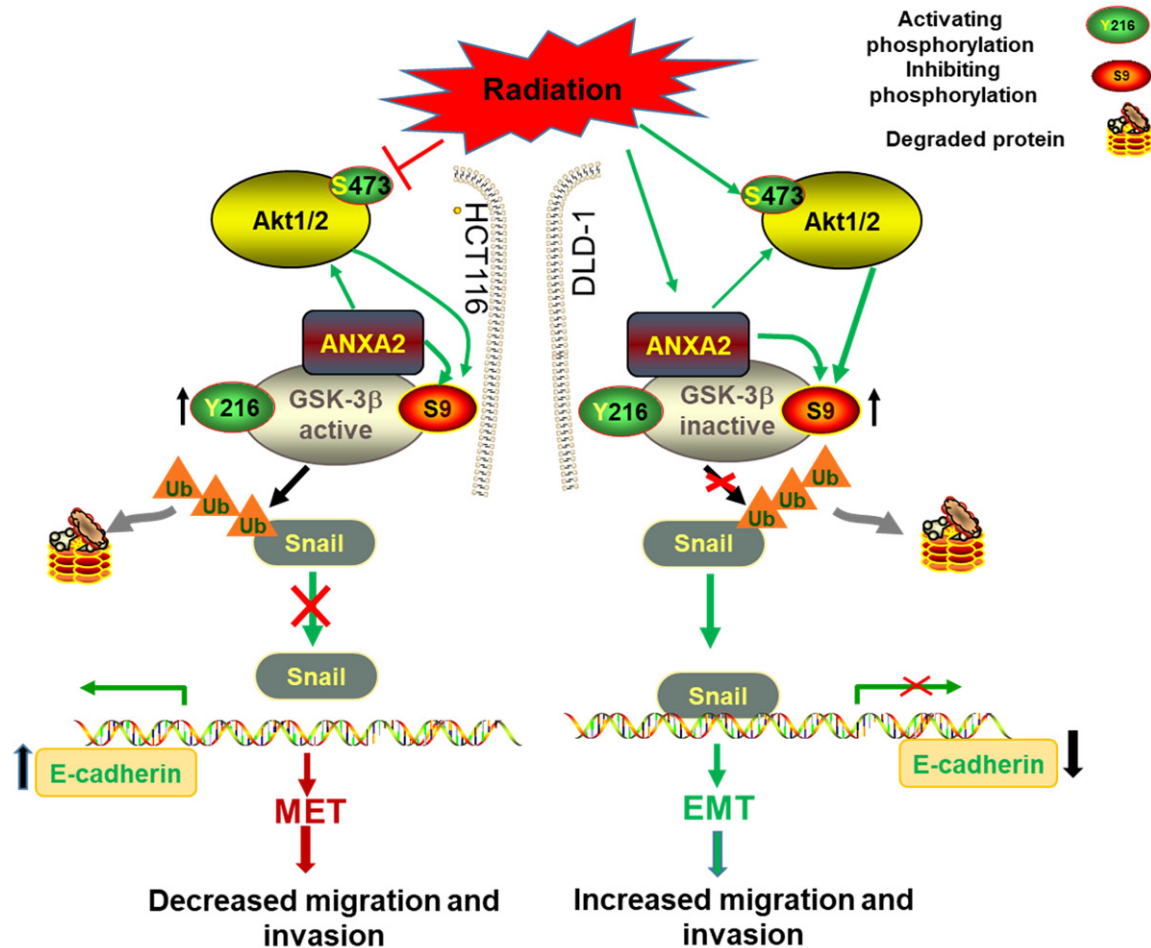


**Figure 8.** Schematic model for radiation induced opposite invasion and migration potential in HCT116 and DLD-1 cells. Radiation increases the phosphorylation of AKT at Ser473 and the expression of ANXA2 overtime in DLD-1 cells, and inactivates GSK3 $\beta$  by up-regulating its phosphorylation at Ser9. The inactive form of GSK3 $\beta$  can't initiate the ubiquitylation of snail, resulting in the accumulation of snail, which promotes EMT process and stimulates the cellular migration and invasion. In HCT116 cells, radiation decreases the phosphorylation of AKT at Ser473 and does not change the expression level of ANXA2, but increases the activation of GSK3 $\beta$  by up-regulating its phosphorylation at Tyr216. The active form of GSK3 $\beta$  promotes the ubiquitylation of snail, results in the increase of E-cadherin expression and finally impairs the cellular migration and invasion.

radiation-enhanced migration in DLD-1 cells but strengthened the radiation-decreased migration in HCT116 cells. Taken together, the above results indicate that the up- or down-regulation of ANXA2 may serve as a biomarker for evaluating the outcome of radiotherapy regarding metastasis and hence is a potential therapeutic target in radiotherapy.

In collusion, this study demonstrated that DLD-1 and HCT116 cells had converse responses to  $\gamma$ -ray or C-ion radiation in cellular migration and invasion both *in vivo* and *in vitro*, which suggests the independence of radiation type on the change of cell motility. We also demonstrated that the opposite cellular motility

ties were resulted from the different EMT or MET process after radiation, which was modulated by AKT/GSK3 $\beta$  signaling pathway. Interestingly, we identified a new regulator of GSK3 $\beta$ , ANXA2, which can directly bind to GSK3 $\beta$  and negatively regulate its activation upon radiation (**Figure 8**). These findings provide a new insight into the mechanism of radiation-altered cell migration and invasion and suggest that ANXA2 is applicable as a potential target of radiotherapy.

### Acknowledgements

This study was mainly supported by the National Natural Science Foundation (Nos. 117-

## Radiation engenders converse migration in different cells

75052, 31770910), Shanghai Science and Technology Commission (No. 19411950902) and the Research Project with Heavy Ions at NIRS-HIMAC of Japan (Proposal Nos. 17J121).

### Disclosure of conflict of interest

None.

**Address correspondence to:** Chunlin Shao and Yan Pan, Institute of Radiation Medicine, Shanghai Medical College, Fudan University, No. 2094 Xie-Tu Road, Shanghai 200032, China. E-mail: clshao@shmu.edu.cn (CLS); swallowpan@fudan.edu.cn (YP)

### References

- [1] Bray F, Ferlay J, Soerjomataram I, Siegel RL, Torre LA and Jemal A. Global cancer statistics 2018: GLOBOCAN estimates of incidence and mortality worldwide for 36 cancers in 185 countries. *CA Cancer J Clin* 2018; 68: 394-424.
- [2] Khatri VP, Petrelli NJ and Belghiti J. Extending the frontiers of surgical therapy for hepatic colorectal metastases: is there a limit? *J Clin Oncol* 2005; 23: 8490-8499.
- [3] Van Cutsem E, Nordlinger B, Adam R, Köhne CH, Pozzo C, Poston G, Ychou M and Rougier P; European Colorectal Metastases Treatment Group. Towards a pan-European consensus on the treatment of patients with colorectal liver metastases. *Eur J Cancer* 2006; 42: 2212-2221.
- [4] Stein A, Atanackovic D and Bokemeyer C. Current standards and new trends in the primary treatment of colorectal cancer. *Eur J Cancer* 2011; 47 Suppl 3: S312-314.
- [5] Kobiela J, Spychalski P, Marvaso G, Ciardo D, Dell'Acqua V, Kraja F, Blazynska-Spychalska A, Lachinski AJ, Surgo A, Glynne-Jones R and Jerezek-Fossa BA. Ablative stereotactic radiotherapy for oligometastatic colorectal cancer: systematic review. *Crit Rev Oncol Hematol* 2018; 129: 91-101.
- [6] Sundahl N, Duprez F, Ost P, De Neve W and Mareel M. Effects of radiation on the metastatic process. *Mol Med* 2018; 24: 16.
- [7] Makishima H, Yasuda S, Isozaki Y, Kasuya G, Okada N, Miyazaki M, Mohamad O, Matsufuji N, Yamada S, Tsuji H and Kamada T; Liver Cancer Working Group. Single fraction carbon ion radiotherapy for colorectal cancer liver metastasis: a dose escalation study. *Cancer Sci* 2019; 110: 303-309.
- [8] Yamada S, Kamada T, Ebner DK, Shinoto M, Terashima K, Isozaki Y, Yasuda S, Makishima H, Tsuji H, Tsujii H, Isozaki T, Endo S, Takahashi K, Sekimoto M, Saito N and Matsubara H; Working Group on Locally Recurrent Rectal Cancer. Carbon-ion radiation therapy for pelvic recurrence of rectal cancer. *Int J Radiat Oncol Biol Phys* 2016; 96: 93-101.
- [9] Eke I, Storch K, Kastner I, Vehlow A, Faethe C, Mueller-Klieser W, Taucher-Scholz G, Temme A, Schackert G and Cordes N. Three-dimensional invasion of human glioblastoma cells remains unchanged by X-ray and carbon ion irradiation in vitro. *Int J Radiat Oncol Biol Phys* 2012; 84: e515-523.
- [10] Fujita M, Otsuka Y, Imadome K, Endo S, Yamada S and Imai T. Carbon-ion radiation enhances migration ability and invasiveness of the pancreatic cancer cell, PANC-1, in vitro. *Cancer Sci* 2012; 103: 677-683.
- [11] de Marcondes PG and Morgado-Diaz JA. The role of EphA4 signaling in radiation-induced EMT-like phenotype in colorectal cancer cells. *J Cell Biochem* 2017; 118: 442-445.
- [12] Zhang H, Song Y, Zhou C, Bai Y, Yuan D, Pan Y and Shao C. Blocking endogenous H2S signaling attenuated radiation-induced long-term metastasis of residual HepG2 cells through inhibition of EMT. *Radiat Res* 2018; 190: 374-384.
- [13] Cui YH, Suh Y, Lee HJ, Yoo KC, Uddin N, Jeong YJ, Lee JS, Hwang SG, Nam SY, Kim MJ and Lee SJ. Radiation promotes invasiveness of non-small-cell lung cancer cells through granulocyte-colony-stimulating factor. *Oncogene* 2015; 34: 5372-5382.
- [14] Kao SH, Wang WL, Chen CY, Chang YL, Wu YY, Wang YT, Wang SP, Nesvizhskii AI, Chen YJ, Hong TM and Yang PC. GSK3beta controls epithelial-mesenchymal transition and tumor metastasis by CHIP-mediated degradation of Slug. *Oncogene* 2014; 33: 3172-3182.
- [15] Zhou BP, Deng J, Xia W, Xu J, Li YM, Gunduz M and Hung MC. Dual regulation of Snail by GSK-3beta-mediated phosphorylation in control of epithelial-mesenchymal transition. *Nat Cell Biol* 2004; 6: 931-940.
- [16] Zheng H, Li W, Wang Y, Liu Z, Cai Y, Xie T, Shi M, Wang Z and Jiang B. Glycogen synthase kinase-3 beta regulates Snail and beta-catenin expression during Fas-induced epithelial-mesenchymal transition in gastrointestinal cancer. *Eur J Cancer* 2013; 49: 2734-2746.
- [17] Ye Y, Xiao Y, Wang W, Yearsley K, Gao JX, Shetuni B and Barsky SH. ERalpha signaling through slug regulates E-cadherin and EMT. *Oncogene* 2010; 29: 1451-1462.
- [18] Sharma MC. Annexin A2 (ANXA2): an emerging biomarker and potential therapeutic target for aggressive cancers. *Int J Cancer* 2019; 144: 2074-2081.

## Radiation engenders converse migration in different cells

- [19] Takano S, Togawa A, Yoshitomi H, Shida T, Kimura F, Shimizu H, Yoshidome H, Ohtsuka M, Kato A, Tomonaga T, Nomura F and Miyazaki M. Annexin II overexpression predicts rapid recurrence after surgery in pancreatic cancer patients undergoing gemcitabine-adjuvant chemotherapy. *Ann Surg Oncol* 2008; 15: 3157-3168.
- [20] Zheng W, Chen Q, Wang C, Yao D, Zhu L, Pan Y, Zhang J, Bai Y and Shao C. Inhibition of Cathepsin D (CTSD) enhances radiosensitivity of glioblastoma cells by attenuating autophagy. *Mol Carcinog* 2020; 59: 651-660.
- [21] Torikoshi M, Minohara S, Kanematsu N, Komori M, Kanazawa M, Noda K, Miyahara N, Itoh H, Endo M and Kanai T. Irradiation system for HIMAC. *J Radiat Res* 2007; 48 Suppl A: A15-25.
- [22] Pan Y, Ye S, Yuan D, Zhang J, Bai Y and Shao C. Radioprotective role of H(2)S/CSE pathway in Chang liver cells. *Mutat Res* 2012; 738-739: 12-18.
- [23] Pan Y, Zhou C, Yuan D, Zhang J and Shao C. Radiation exposure promotes hepatocarcinoma cell invasion through epithelial mesenchymal transition mediated by H2S/CSE pathway. *Radiat Res* 2016; 185: 96-105.
- [24] Pan Y, Ye S, Yuan D, Zhang J, Bai Y and Shao C. Hydrogen sulfide (H2S)/cystathionine gamma-lyase (CSE) pathway contributes to the proliferation of hepatoma cells. *Mutat Res* 2014; 763-764: 10-18.
- [25] Li H, Rokavec M, Jiang L, Horst D and Hermeking H. Antagonistic effects of p53 and HIF1A on microRNA-34a regulation of PPP1R11 and STAT3 and hypoxia-induced epithelial to mesenchymal transition in colorectal cancer cells. *Gastroenterology* 2017; 153: 505-520.
- [26] Vilalta M, Rafat M and Graves EE. Effects of radiation on metastasis and tumor cell migration. *Cell Mol Life Sci* 2016; 73: 2999-3007.
- [27] Wozny AS, Vares G, Alphonse G, Lauret A, Monini C, Magne N, Cuerq C, Fujimori A, Monboisse JC, Beuve M, Nakajima T and Rodriguez-Lafrasse C. ROS production and distribution: a new paradigm to explain the differential effects of X-ray and carbon ion irradiation on cancer stem cell migration and invasion. *Cancers (Basel)* 2019; 11: 468.
- [28] Fujita M, Imadome K, Shoji Y, Isozaki T, Endo S, Yamada S and Imai T. Carbon-ion irradiation suppresses migration and invasiveness of human pancreatic carcinoma cells MIAPaCa-2 via Rac1 and RhoA degradation. *Int J Radiat Oncol Biol Phys* 2015; 93: 173-180.
- [29] Goetze K, Scholz M, Taucher-Scholz G and Mueller-Klieser W. The impact of conventional and heavy ion irradiation on tumor cell migration in vitro. *Int J Radiat Biol* 2007; 83: 889-896.
- [30] Konings K, Belmans N, Vermeesen R, Baselet B, Lamers G, Janssen A, Isebaert S, Baatout S, Haustermans K and Moreels M. Targeting the Hedgehog pathway in combination with X-ray or carbon ion radiation decreases migration of MCF7 breast cancer cells. *Int J Oncol* 2019; 55: 1339-1348.
- [31] Murata K, Noda SE, Oike T, Takahashi A, Yoshida Y, Suzuki Y, Ohno T, Funayama T, Kobayashi Y, Takahashi T and Nakano T. Increase in cell motility by carbon ion irradiation via the Rho signaling pathway and its inhibition by the ROCK inhibitor Y-27632 in lung adenocarcinoma A549 cells. *J Radiat Res* 2014; 55: 658-664.
- [32] Karger CP, Scholz M, Huber PE, Debus J and Peschke P. Photon and carbon ion irradiation of a rat prostate carcinoma: does a higher fraction number increase the metastatic rate? *Radiat Res* 2014; 181: 623-628.
- [33] Lee SY, Jeong EK, Ju MK, Jeon HM, Kim MY, Kim CH, Park HG, Han SI and Kang HS. Induction of metastasis, cancer stem cell phenotype, and oncogenic metabolism in cancer cells by ionizing radiation. *Mol Cancer* 2017; 16: 10.
- [34] Puisieux A, Brabletz T and Caramel J. Oncogenic roles of EMT-inducing transcription factors. *Nat Cell Biol* 2014; 16: 488-494.
- [35] Thiery JP, Acloque H, Huang RY and Nieto MA. Epithelial-mesenchymal transitions in development and disease. *Cell* 2009; 139: 871-890.
- [36] Zhu Y, Wang C, Becker SA, Hurst K, Nogueira LM, Findlay VJ and Camp ER. miR-145 antagonizes SNAI1-mediated stemness and radiation resistance in colorectal cancer. *Mol Ther* 2018; 26: 744-754.
- [37] Li S, Lu J, Chen Y, Xiong N, Li L, Zhang J, Yang H, Wu C, Zeng H and Liu Y. MCP-1-induced ERK/GSK-3beta/Snail signaling facilitates the epithelial-mesenchymal transition and promotes the migration of MCF-7 human breast carcinoma cells. *Cell Mol Immunol* 2017; 14: 621-630.
- [38] Cheng S, Qian F, Huang Q, Wei L, Fu Y and Du Y. HOXA4, down-regulated in lung cancer, inhibits the growth, motility and invasion of lung cancer cells. *Cell Death Dis* 2018; 9: 465.
- [39] Jiang H, Guo W, Liang X and Rao Y. Both the establishment and the maintenance of neuronal polarity require active mechanisms: critical roles of GSK-3beta and its upstream regulators. *Cell* 2005; 120: 123-135.
- [40] Hughes K, Nikolakaki E, Plyte SE, Totty NF and Woodgett JR. Modulation of the glycogen synthase kinase-3 family by tyrosine phosphorylation. *EMBO J* 1993; 12: 803-808.
- [41] Nagarajan D, Melo T, Deng Z, Almeida C and Zhao W. ERK/GSK3beta/Snail signaling mediates radiation-induced alveolar epithelial-to-

## Radiation engenders converse migration in different cells

- mesenchymal transition. *Free Radic Biol Med* 2012; 52: 983-992.
- [42] Yan X, Zhang D, Wu W, Wu S, Qian J, Hao Y, Yan F, Zhu P, Wu J, Huang G, Huang Y, Luo J, Liu X, Liu B, Chen X, Du Y, Chen R and Fan Z. Mesenchymal stem cells promote hepatocarcinogenesis via lncRNA-MUF interaction with ANXA2 and miR-34a. *Cancer Res* 2017; 77: 6704-6716.
- [43] Castaldo SA, Ajime T, Serrao G, Anastacio F, Rosa JT, Giacomantonio CA, Howarth A, Hill R and Madureira PA. Annexin A2 regulates AKT upon H(2)O(2)-dependent signaling activation in cancer cells. *Cancers (Basel)* 2019; 11: 492.
- [44] D'Souza S, Kurihara N, Shiozawa Y, Joseph J, Taichman R, Galson DL and Roodman GD. Annexin II interactions with the annexin II receptor enhance multiple myeloma cell adhesion and growth in the bone marrow microenvironment. *Blood* 2012; 119: 1888-1896.
- [45] Zhang L, Ge C, Zhao F, Zhang Y, Wang X, Yao M and Li J. NRBP2 overexpression increases the chemosensitivity of hepatocellular carcinoma cells via akt signaling. *Cancer Res* 2016; 76: 7059-7071.
- [46] Jurcak NR, Rucki AA, Muth S, Thompson E, Sharma R, Ding D, Zhu Q, Eshleman JR, Anders RA, Jaffee EM, Fujiwara K and Zheng L. Axon guidance molecules promote perineural invasion and metastasis of orthotopic pancreatic tumors in mice. *Gastroenterology* 2019; 157: 838-850, e836.
- [47] Sharma MR, Koltowski L, Ownbey RT, Tuszynski GP and Sharma MC. Angiogenesis-associated protein annexin II in breast cancer: selective expression in invasive breast cancer and contribution to tumor invasion and progression. *Exp Mol Pathol* 2006; 81: 146-156.

## Radiation engenders converse migration in different cells

**Supplementary Table 1.** Identification of proteins interacting with GSK3beta by mass spectrometry

Protein IDs	Gene Name	Number of proteins	Peptides	unique peptides	Sequence coverage [%]	MW [kDa]	LFQ intensity HCT116-1	LFQ intensity HCT116-2	LFQ intensity DLD1-1	LFQ intensity DLD1-2
P0DOX8	IGLL5	6	3	2	14.4	22.83	3.6E+09	2E+09	2.2E+09	3.6E+09
P63261	ACTG1	12	16	16	61.1	41.792	1.1E+09	1.5E+08	1.5E+08	3.62E+08
P35579	MYH9	3	22	19	10.7	226.53	0	917260	1205100	3035500
P18124	RPL7	1	13	13	26.6	29.225	1.7E+08	1.6E+09	3.1E+08	3.7E+08
P84098	RPL19	1	7	7	23	23.466	6.5E+08	9.8E+08	2.1E+08	5.03E+08
P35580	MYH10	1	17	13	8.1	229	0	0	0	0
Q5VTE0	EEF1A1P5	3	6	6	16.7	50.184	8.9E+07	1.5E+08	1.1E+08	1.26E+08
Q6NXT2	H3F3C	5	2	2	11.9	15.214	7.9E+07	1.1E+08	1.1E+08	1.21E+08
Q07020	RPL18	1	5	5	26.1	21.634	6.9E+07	1.8E+08	7.4E+07	52467000
P08238	HSP90AB1	2	7	4	9.4	83.263	1.1E+08	8.6E+07	4.8E+07	46220000
P62917	RPL8	1	5	5	19.8	28.024	1.4E+08	1.3E+08	5.8E+07	1.2E+08
P36578	RPL4	1	3	3	6.6	47.697	9.3E+07	9.3E+07	6E+07	1.3E+08
Q00839	HNRNPU	1	8	8	8.7	90.583	1.5E+08	1.1E+08	1.2E+08	46728000
P04406	GAPDH	2	6	6	16.7	36.053	5.7E+07	7.6E+07	4.2E+07	52582000
P26373	RPL13	1	8	8	26.5	24.261	1.5E+08	1.1E+08	6.3E+07	1.38E+08
Q02878	RPL6	1	5	5	14.6	32.728	4.5E+07	7.2E+07	4.1E+07	44051000
P06748	NPM1	1	3	3	10.5	32.575	9E+07	7.2E+07	9.7E+07	1.07E+08
P16403	HIST1H1C	6	8	8	31.9	21.364	5.3E+07	2E+08	9.5E+07	92712000
P05141	SLC25A5	4	3	3	8.4	32.852	5.5E+07	6.3E+07	3.5E+07	43005000
P61254	RPL26	2	4	4	17.9	17.258	7.7E+07	4.7E+07	3.9E+07	0
P46779	RPL28	1	4	4	21.9	15.747	1E+08	5.4E+07	3.9E+07	90432000
P62826	RAN	1	4	4	14.4	24.423	3.1E+07	6.4E+07	3.2E+07	53773000
Q9BQE3	TUBA1C	9	2	2	4.2	49.895	9.2E+07	4.8E+07	1.8E+07	0
AOA075B6IO	IGLV8-61	1	2	2	13.1	12.814	0	1.2E+08	1.3E+08	1.58E+08
P18621	RPL17	1	2	2	10.3	21.397	5.3E+07	4.4E+07	2.4E+07	29591000
P06733	ENO1	1	3	3	3.9	47.168	2.9E+07	2E+07	2.4E+07	55982000
P39023	RPL3	1	4	4	8.9	46.108	3.5E+07	4.9E+07	2.8E+07	0
P61313	RPL15	1	3	3	16.7	24.146	0	6.8E+07	1.9E+07	31254000
P15924	DSP	1	16	16	5.2	331.77	6.7E+07	3.5E+07	9.4E+07	1.07E+08
P62701	RPS4X	3	4	4	14.4	29.597	0	7.6E+07	0	0
P62805	HIST1H4A	1	3	3	31.1	11.367	0	2.1E+07	3.5E+07	13250000
P07437	TUBB	9	4	1	9.9	49.67	2.2E+07	5.8E+07	3.8E+07	29222000
P38646	HSPA9	1	6	6	9.6	73.68	3.3E+07	3.2E+07	1.3E+07	23541000
P62424	RPL7A	1	5	5	19.2	29.995	1.1E+07	6.3E+07	3.4E+07	0

## Radiation engenders converse migration in different cells

P00338	LDHA	3	3	2	9.3	36.688	3.1E+07	4.2E+07	0	0
P63104	YWHAZ	1	5	5	25.3	27.745	2E+07	2.2E+07	1E+07	32793000
P67809	YBX1	3	5	5	24.4	35.924	2.1E+07	3.4E+07	1.7E+07	27430000
P07900	HSP90AA1	3	5	3	6.7	84.659	2.1E+07	1.6E+07	0	15053000
P61247	RPS3A	1	5	5	13.6	29.945	5.4E+07	4.2E+07	2.3E+07	29312000
P07355	ANXA2	2	3	3	10.9	38.604	0	1.5E+07	1.7E+07	22624000
P62269	RPS18	1	5	5	28.9	17.718	0	3.1E+07	2E+07	30486000
P25705	ATP5F1A	1	6	6	9.9	59.75	0	5.5E+07	1.4E+07	11000000
P07195	LDHB	1	4	3	13.5	36.638	2.1E+07	1.7E+07	1.5E+07	17318000
P17066	HSPA6	2	2	1	2.8	71.027	1.7E+07	1.8E+07	1.3E+07	28337000
Q99623	PHB2	1	2	2	7	33.296	0	0	0	0
P46781	RPS9	1	3	3	13.9	22.591	0	4.6E+07	1.8E+07	0
P78527	PRKDC	1	2	2	0.4	469.08	1E+07	1.2E+07	1.6E+07	0
P62750	RPL23A	1	6	6	34	17.695	1.5E+07	4.9E+07	1.4E+07	12123000
P14923	JUP	1	5	5	7	81.744	1.9E+07	0	1.8E+07	22084000
P62851	RPS25	1	2	2	12.8	13.742	1.3E+07	2.8E+07	1.3E+07	0
P00387	CYB5R3	1	2	2	6.3	34.234	1.1E+07	1.4E+07	0	0
P14618	PKM	1	3	3	5.3	57.936	1.6E+07	1.5E+07	1.7E+07	31628000
P07305	H1FO	1	3	3	15.5	20.863	1.7E+07	2.9E+07	3473100	8618900
P61353	RPL27	1	2	2	14	15.798	6871300	1.2E+07	8030200	0
P69905	HBA1	1	1	1	10.6	15.257	0	2.1E+07	0	0
P62753	RPS6	1	4	4	8	28.68	0	7.9E+07	0	35219000
P62241	RPS8	1	2	2	5.8	24.205	0	2E+07	5639700	0
Q8NC51	SERBP1	1	2	2	7.1	44.965	1.4E+07	8444000	0	11926000
Q9Y623	MYH4	1	7	2	3.6	223.07	0	1.4E+07	4.3E+07	0
P83731	RPL24	1	3	3	19.1	17.779	0	1.2E+07	3718400	0
O60506	SYNCRIP	2	3	3	4.8	69.602	3484800	3648500	2242200	0
P62277	RPS13	1	3	3	14.6	17.222	0	9066600	7253800	0
Q9Y3Y2	CHTOP	1	1	1	5.2	26.396	0	0	0	3294200
Q9UL25	RAB21	1	1	1	6.7	24.347	0	0	0	2337300
Q9UIF9	BAZ2A	1	1	1	0.5	211.2	0	0	0	1.19E+09
Q9UBN4	TRPC4	1	1	1	1.1	112.1	0	0	0	74121000
Q9P2F5	STOX2	1	1	1	1.5	102.67	0	0	0	30720000
Q9NUL3	STAU2	2	1	1	1.4	62.608	0	0	0	0
Q9BWG4	SSBP4	1	1	1	3.4	39.388	0	0	0	27295000
Q9BV35	SLC25A23	2	1	1	1.7	52.377	0	0	0	2815100

Radiation engenders converse migration in different cells

Q99879	HIST1H2BM	16	3	3	25.4	13.989	1.1E+07	0	0	0
Q99832	CCT7	1	1	1	1.7	59.366	0	0	0	4013900
Q96H10	SENP5	1	1	1	1.2	86.692	0	0	0	0
Q8TF72	SHROOM3	1	1	1	0.5	216.85	0	0	0	3.09E+08
Q8TE56	ADAMTS17	1	1	1	0.8	121.13	0	0	0	1.49E+08
Q8TAL5	C9orf43	1	1	1	2	52.221	0	0	0	0
Q8NHW5	RPLP0P6	2	1	1	3.5	34.364	0	0	0	11097000
Q8N9V2	TRIML1	1	1	1	1.9	53.001	0	0	0	0
Q86SZ2	TRAPPC6B	1	1	1	8.9	17.983	0	0	0	14821000
Q86SG5	S100A7A	2	1	1	6.9	11.305	0	0	0	0
Q6ZUT6	CCDC9B	1	1	1	1.5	57.324	0	0	0	0
Q5T749	KPRP	1	1	1	1.6	64.135	0	0	0	5861200
Q14166	TLL12	1	1	1	1.1	74.403	0	0	0	93348000
Q13200	PSMD2	1	1	1	1.3	100.2	0	0	0	0
Q12906	ILF3	2	2	2	2.7	95.337	0	0	2565000	0
Q08554	DSC1	1	2	2	2.7	99.986	0	0	0	2628400
Q08493	PDE4C	1	1	1	1	79.901	0	0	0	3.48E+08
Q08188	TGM3	1	1	1	1.3	76.631	0	0	0	9354300
Q03252	LMNB2	1	3	3	5.8	69.948	0	1.1E+07	0	0
Q02543	RPL18A	1	2	2	10.2	20.762	0	2E+07	1E+07	0
Q02413	DSG1	1	3	3	3.2	113.75	0	0	1.5E+07	13083000
Q01469	FABP5	1	1	1	6.7	15.164	0	0	0	2746700
Q01105	SET	2	1	1	4.5	33.488	0	0	0	2931900
Q00325	SLC25A3	1	1	1	3.3	40.094	0	0	0	0
P83881	RPL36A	1	1	1	9.4	12.441	0	0	0	8096400
P81605	DCD	1	3	3	27.3	11.284	0	0	3.4E+07	0
P68371	TUBB4B	1	4	1	9.9	49.83	0	0	3101300	0
P63244	RACK1	1	1	1	3.2	35.076	0	0	0	8940900
P62937	PPIA	1	1	1	11.5	18.012	0	0	0	0
P62906	RPL10A	1	1	1	3.7	24.831	0	0	0	16444000
P62899	RPL31	1	1	1	7.2	14.463	0	0	0	15063000
P62280	RPS11	1	2	2	11.4	18.431	0	0	0	0
P62258	YWHAE	1	1	1	4.3	29.174	0	0	0	0
P62195	PSMC5	1	1	1	3.7	45.626	0	0	0	4168100
P55795	HNRNPH2	2	1	1	3.6	49.263	0	0	0	0
P54886	ALDH18A1	1	2	2	2.4	87.301	0	0	0	5.12E+09

Radiation engenders converse migration in different cells

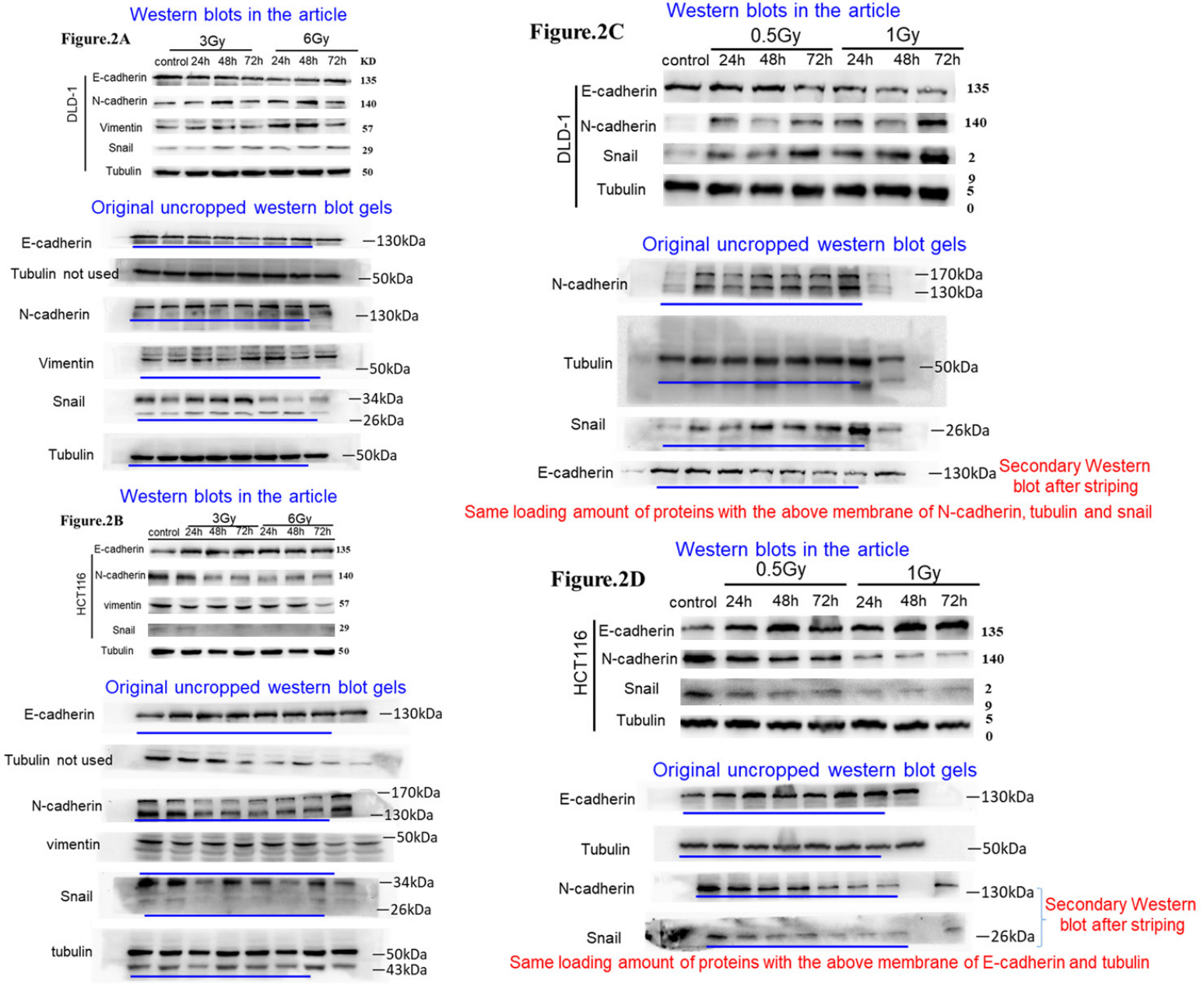
P53999	SUB1	1	1	1	8.7	14.395	0	0	1133800	0
P51512	MMP16	1	1	1	1.5	69.521	0	0	0	0
P50991	CCT4	1	1	1	2	57.924	9659600	0	0	0
P50914	RPL14	1	1	1	5.6	23.432	0	0	1553700	0
P49841	GSK3B	1	2	2	7.4	46.744	0	0	0	10492000
P49411	TUFM	1	2	2	5.1	49.541	0	0	0	3116000
P47914	RPL29	1	1	1	9.4	17.752	0	0	0	25682000
P46777	RPL5	1	2	2	6.1	34.362	0	0	0	10828000
P46776	RPL27A	1	1	1	7.4	16.561	0	0	0	5953500
P40429	RPL13A	2	3	3	11.3	23.577	0	0	1.3E+07	0
P40227	CCT6A	1	2	2	3.4	58.024	0	0	0	1502300
P35232	PHB	1	2	2	6.6	29.804	0	0	0	8358400
P35030	PRSS3	1	1	1	4.3	32.528	0	0	0	0
P32969	RPL9	1	1	1	4.2	21.863	0	0	0	5524600
P30050	RPL12	1	2	2	10.3	17.818	0	0	0	14744000
P27635	RPL10	1	1	1	4.2	24.604	0	0	0	0
P27348	YWHAQ	1	1	1	5.7	27.764	0	0	0	0
P25311	AZGP1	1	1	1	3.4	34.258	0	0	0	8412300
P23528	CFL1	1	1	1	7.2	18.502	0	1.1E+07	0	0
P23396	RPS3	1	3	3	12.3	26.688	1.6E+07	2.5E+07	0	5492000
P19338	NCL	1	2	2	3	76.613	0	0	0	0
P15311	EZR	1	2	2	2.7	69.412	0	8258500	0	0
P15090	FABP4	1	2	2	12.9	14.719	0	0	1.8E+07	0
P13010	XRCC5	1	2	2	2	82.704	0	0	7705600	0
P12268	IMPDH2	1	1	1	2.3	55.804	0	0	0	5305000
P11387	TOP1	1	2	2	3	90.725	0	7401100	0	0
P10809	HSPD1	1	2	2	3.7	61.054	1.2E+07	0	0	0
P10599	TXN	1	1	1	8.6	11.737	0	0	0	7783200
P09651	HNRNPA1	1	1	1	4.8	38.746	0	0	0	3829200
P09493	TPM1	2	1	1	3.2	32.708	0	0	0	0
P08670	VIM	2	7	4	11.6	53.651	0	2424500	1.2E+07	0
P08254	MMP3	1	1	1	1.9	53.977	0	0	0	0
P07910	HNRNPC	5	4	4	9.8	33.67	0	3.2E+07	2.3E+07	28689000
P06576	ATP5F1B	1	1	1	2.3	56.559	0	0	567990	0
P06312	IGKV4-1	1	1	1	5.8	13.38	0	0	0	1.11E+08
P05976	MYL1	2	1	1	4.6	21.145	0	0	0	0

### Radiation engenders converse migration in different cells

P04279	SEMG1	2	2	2	7.4	52.13	0	0	0	3109200
P04083	ANXA1	1	1	1	3.2	38.714	0	0	0	0
P04075	ALDOA	1	5	5	15.4	39.42	0	0	0	0
P02545	LMNA	1	2	2	3.6	74.139	1.2E+07	1E+07	0	0
P01857	IGHG1	5	2	2	5.8	36.105	0	0	0	0
P01834	IGKC	2	1	1	18.7	11.765	0	0	0	0
P01624	IGKV3-15	2	1	1	7.8	12.496	0	0	0	47240000
P01615	IGKV2D-28	4	1	1	5.8	12.957	0	0	0	5.47E+09
O95996	APC2	1	1	1	0.4	243.95	0	0	0	1.32E+09
O75874	IDH1	1	2	2	5.1	46.659	0	0	0	0
O15523	DDX3Y	2	2	2	3.3	73.153	0	0	0	2.2E+07
O00425	IGF2BP3	1	1	1	1.6	63.704	9163800	0	0	0

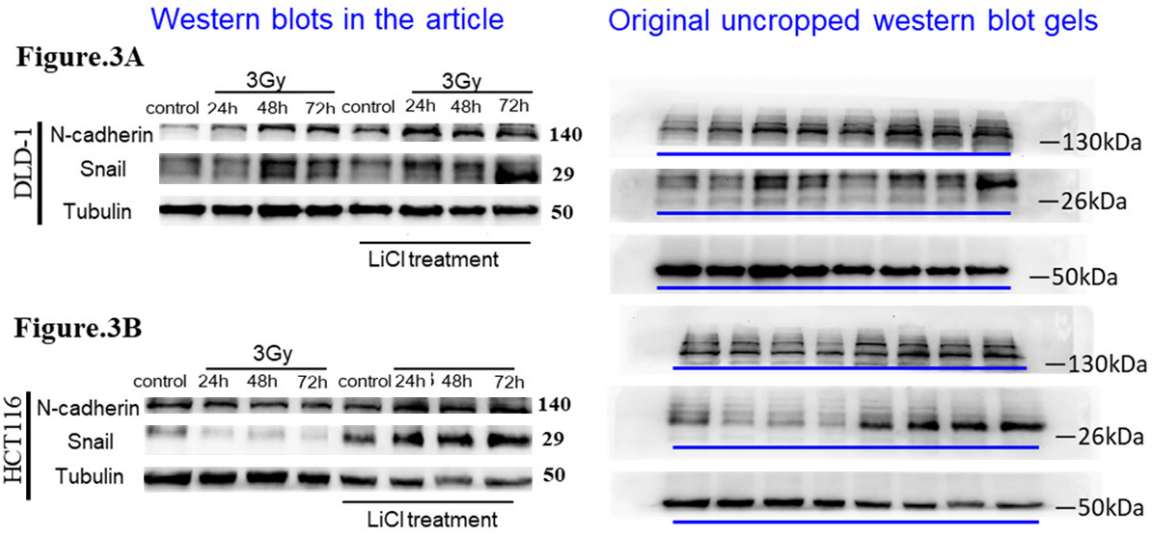
HCT116-1: proteins from HCT116 cells with no radiation; HCT116-2: proteins from HCT116 cells with 3 Gy of  $\gamma$ -radiation; DLD-1-1: proteins from DLD-1 cells with no radiation; DLD-1-2: proteins from DLD-1 cells with 3 Gy of  $\gamma$ -radiation.

# Radiation engenders converse migration in different cells



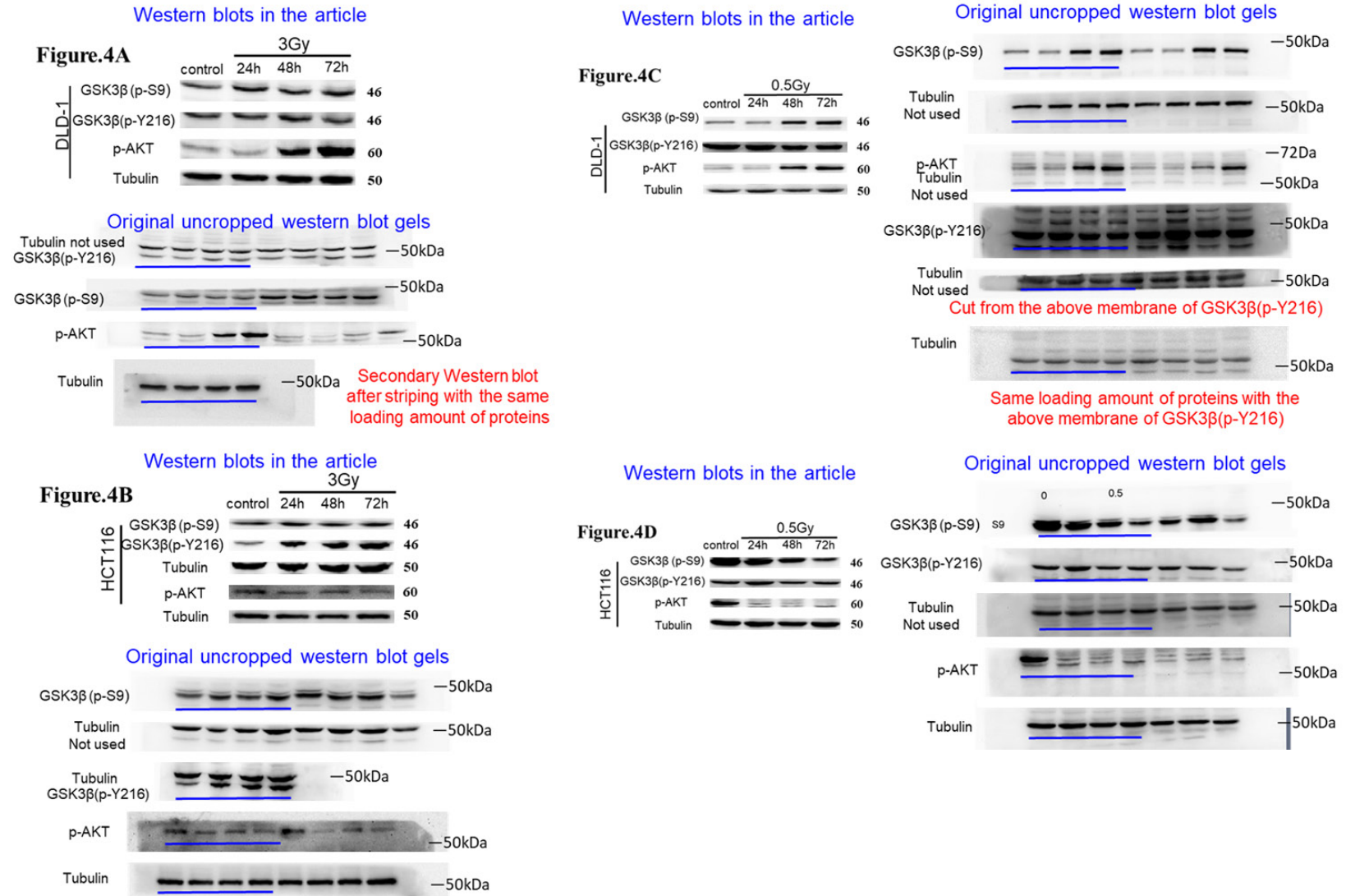
Supplementary Figure 1. The original uncropped gels for Western blots in Figure 2.

Radiation engenders converse migration in different cells



Supplementary Figure 2. The original uncropped gels for western blots in Figure 3.

Radiation engenders converse migration in different cells



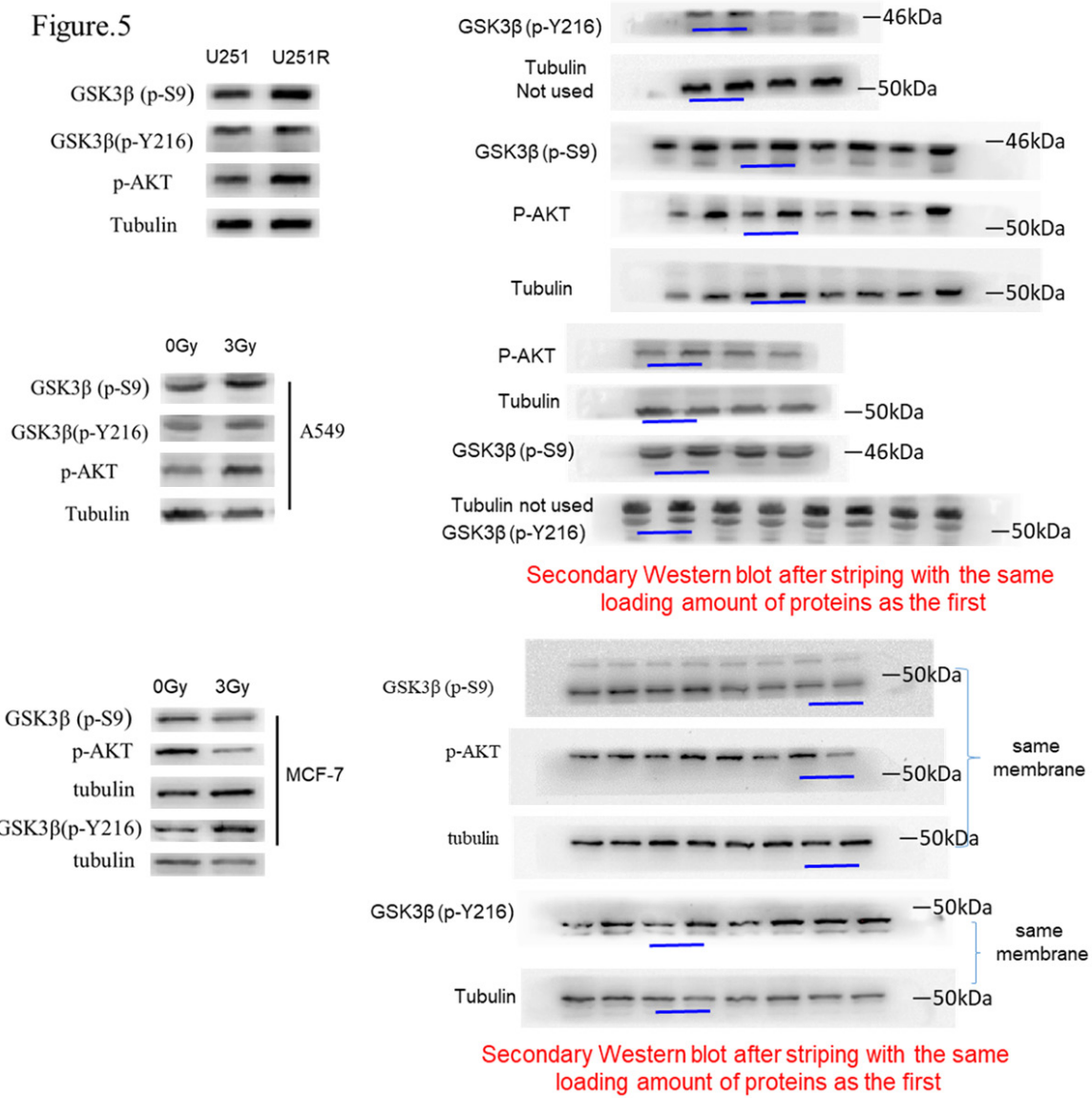
Supplementary Figure 3. The original uncropped gels for western blots in Figure 4.

Radiation engenders converse migration in different cells

Western blots in the article

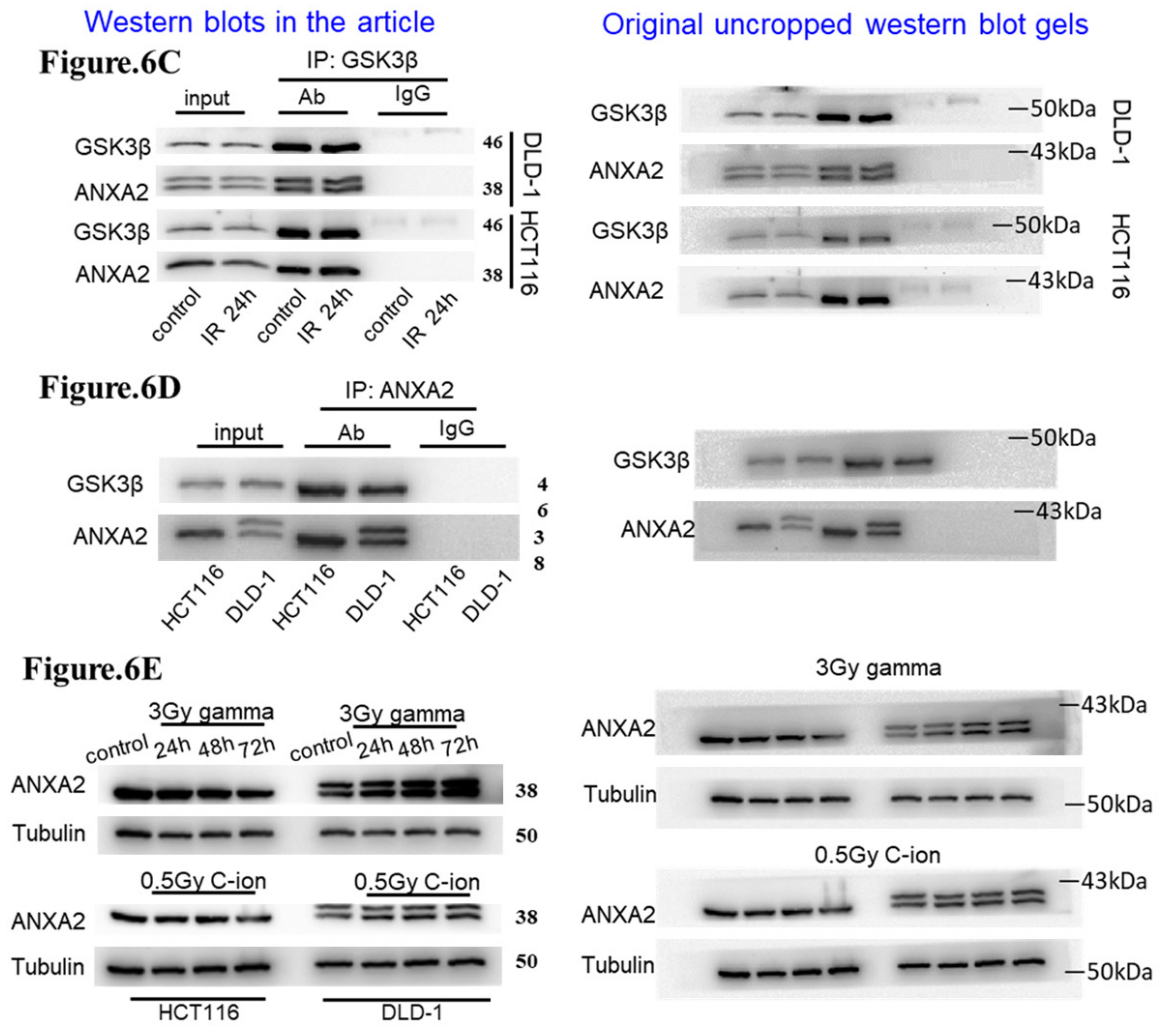
Original uncropped western blot gels

Figure.5



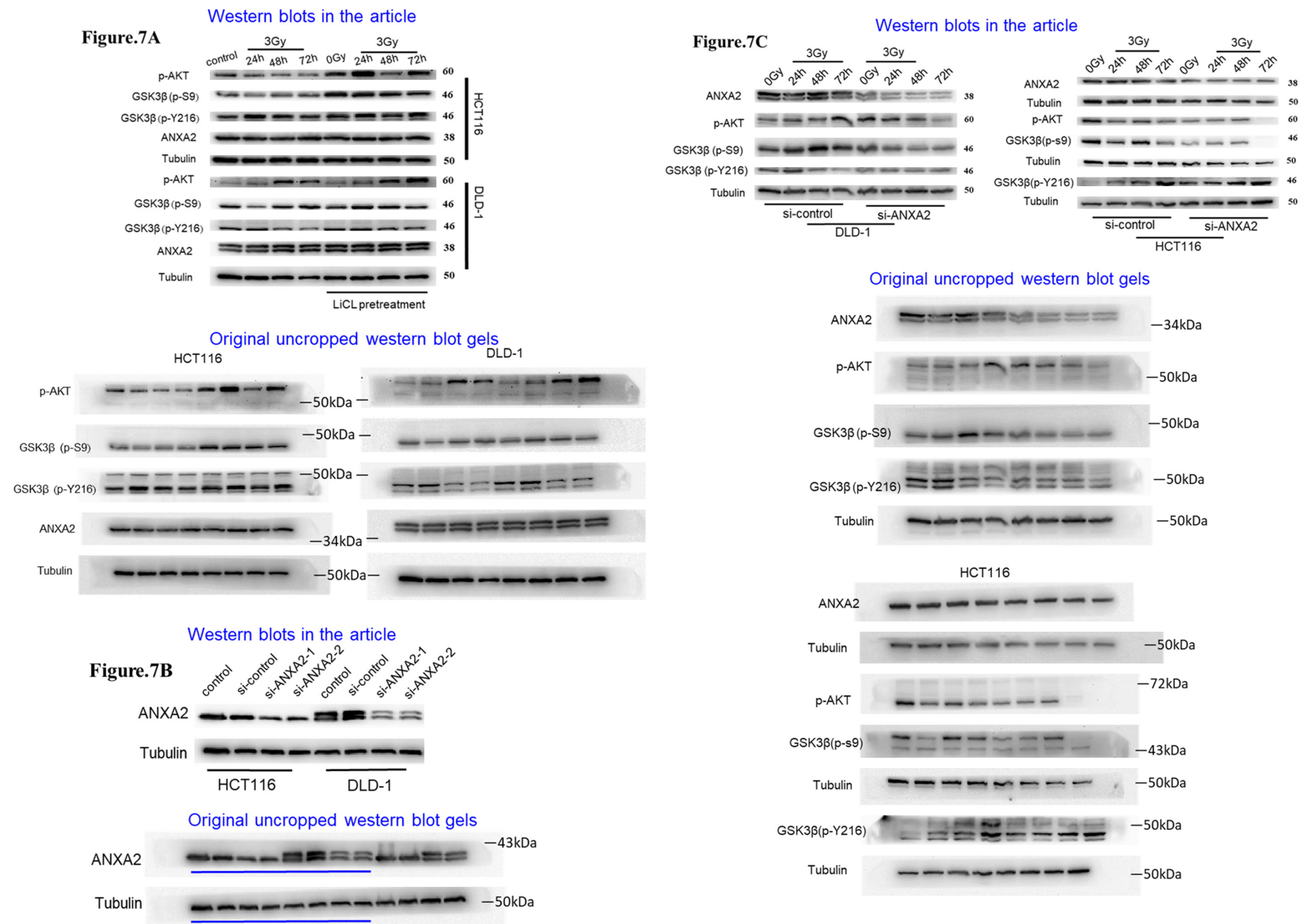
Supplementary Figure 4. The original uncropped gels for western blots in Figure 5.

Radiation engenders converse migration in different cells



Supplementary Figure 5. The original uncropped gels for western blots in Figure 6.

# Radiation engenders converse migration in different cells



Supplementary Figure 6. The original uncropped gels for western blots in Figure 7.